

## TAB: Transformer Attention Bottlenecks enable User Intervention and Debugging in Vision-Language Models

Pooyan Rahmazadehgrevi<sup>†</sup>

pooyan.rmz@gmail.com

Hung Huy Nguyen<sup>†</sup>

hhn0008@auburn.edu

Rosanne Liu<sup>♣</sup>

mimosavvy@gmail.com

Long Mai<sup>◊</sup>

mai.t.long88@gmail.com

<sup>†</sup> Auburn University

Anh Totti Nguyen<sup>†</sup>

anh.ng8@gmail.com

<sup>♣</sup> Google DeepMind, ML Collective

<sup>◊</sup> Adobe Research

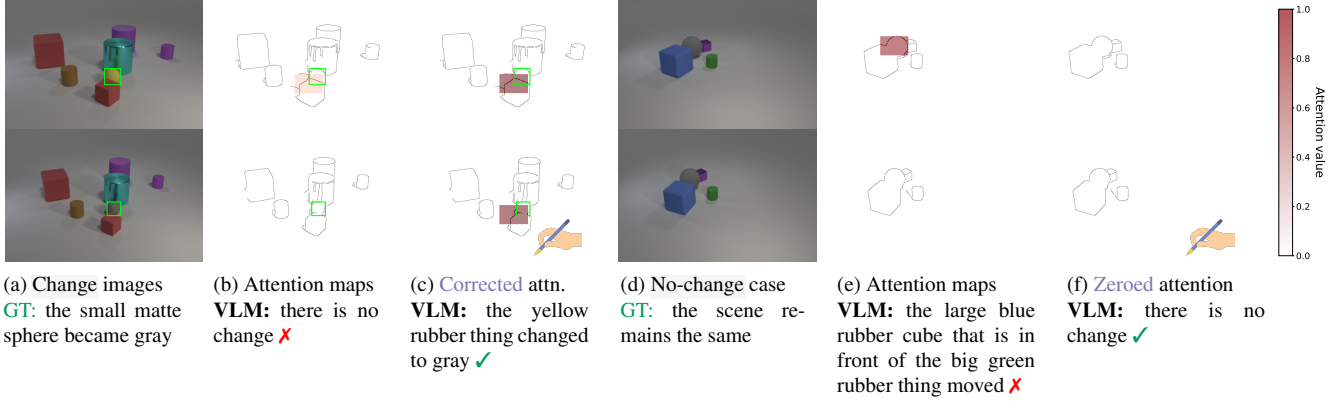


Figure 1. Our bottleneck attention maps (b) & (e) faithfully show the visual patches that contribute to the output of a vision-language model, trained to caption differences (here, across CLEVR-Change image pairs). Users can adjust the attention values, guiding the VLM to attend to the correct objects (c) or to ignore all patches (f), leading to more accurate generated captions ✓.

## Abstract

*Multi-head self-attention (MHSA) is a key component of Transformers [59], a widely popular architecture in both language and vision. Multiple heads intuitively enable different parallel processes over the same input. Yet, they also obscure the attribution of each input patch to the output of a model [7, 14]. We propose a novel 1-head Transformer Attention Bottleneck (TAB) layer, inserted after the traditional MHSA architecture, to serve as an attention bottleneck for interpretability and intervention. Unlike standard self-attention [59], TAB constrains the total attention over all patches to  $\in [0, 1]$ . That is, when the total attention is 0, no visual information is propagated further into the network and the vision-language model (VLM) would default to a generic, image-independent response (Fig. 1f). To demonstrate the advantages of TAB, we train VLMs with TAB to perform image difference captioning. Over three datasets, our models perform similarly to baseline VLMs in captioning but the bottleneck is **superior in localizing** changes and in identifying when no changes occur. TAB is the first ar-*

**chitecture to enable users to intervene** by editing attention, which often produces expected outputs by VLMs.

## 1. Introduction

Vision Transformers (ViTs) [19] are the backbone architecture of modern image classifiers and VLMs. Yet, it is unknown which exact image patches a ViT focuses on and how they contribute to model predictions [14], because the attention heads in a multi-head self-attention (MHSA) block often exhibit various matching patterns, and attention maps may diffuse across the entire image [16]. Attribution methods [7, 14, 16] must compress over a hundred attention maps (e.g., 12 layers  $\times$  12 heads = 144 heads in ViT-B/32 [19]) into a single attribution heatmap that often has little utility [42]. First, in most vision tasks, there is no groundtruth for evaluating attribution maps [7]. Second, even when highlighting salient objects, an attribution map may not actually help users much in decision-making [42]. Third, given a large set of 144 attention maps, it is unknown how a user could guide VLMs on where to look, at either

training or test time.

To address the above three problems, we propose TAB, a novel, 1-head co-attention [38] layer, inserted after the standard MHSA blocks [59], to serve as a bottleneck that (1) shows exact per-patch attention values, requiring no post-hoc processing; (2) can be supervised with groundtruth bounding-box annotations during training; and (3) can be edited by users (Fig. 1c) at test time for debugging or human-machine collaboration.

In this work, we test TAB in VLMs trained to caption changes given two input images. Change captioning is an ideal application for TAB because (1) groundtruth attention maps are available; (2) the attention bottleneck directly filters the visual information that flows into the language model, and therefore editing visual attention has a meaningful, direct impact on a VLM’s responses (Fig. 2).

Change captioning (CC) has a wide range of applications including remote sensing [20, 25], camera surveillance [27], medical imaging [26, 32, 39], urban planning [56], and describing birds [63, 64] or photo edits [11, 58]. CC methods [47, 51, 64] often rely on post-hoc techniques to visualize their ViT attention and do not offer any mechanism for editing attention at test time. We insert TAB into a state-of-the-art (SotA) VLM [23] and train it for change captioning. Our experiments on three different benchmarks show that:<sup>1</sup>

- With TAB, VLMs outperform their direct no-TAB baselines [23] and other ViT-based models consistently on three **captioning** benchmarks (Sec. 5.1).
- In addition to a standard captioning loss, we supervise the attention in TAB using groundtruth bounding-box annotations enabling TAB to be superior in localizing changes to the common MHSA attention of ViTs (Sec. 5.2).
- Our test-time **intervention** experiments show strong causality between the attention values in TAB and VLM responses (Sec. 5.3). That is, editing TAB to focus on objects corresponding to human-annotated changes causes VLMs to improve captions (Fig. 1c). In contrast, zeroing out the attention in TAB will always result in a generic “there is no change” response by VLMs (Fig. 1f).
- Interestingly, the TAB of our VLM trained on OpenImages-I [43] localizes changes on an *unseen* multi-change dataset (Spot-the-Diff [27]) remarkably well—better than baseline VLMs without TAB [23] and only slightly worse than a SotA detector [53] (Sec. 5.4).

## 2. Related Work

**ViT attention visualization** Many feature attribution methods for ViTs aggregate attention heads across all layers into a single heatmap using linear weights computed via gradients [14, 55] or heuristics [4, 16, 50]. Other approaches visualize the similarity scores between text and

image tokens [29, 54]. However, these methods can be unreliable [7, 44] and may not provide meaningful utility to users [42]. In contrast, TAB eliminates the need for post-processing and is the first approach to enable users to intervene on an attention map at test time.

**Class embeddings** On top of image patches, ViTs include an extra [CLS] token [19]. Consequently, the largest ViT, *i.e.*  $14 \times 14$ px patches on  $224 \times 224$  images, generates 256 image patches plus the [CLS] as the final representation of the input image. In each attention head, the *softmax* function sums to 1 over all 257 patches. Prior works [10, 65] showed that using global average pooling, instead of adding the [CLS], can sufficiently aggregate the embeddings from image patches to represent the images, which also improves the scalability and the memory usage of ViTs [65]. In our CC setup, we visualize the **attention** values (Fig. 2) for both change and no-change pairs, and desire an empty, all-zero attention map for no-change pairs, *i.e.*, all image patches should have 0 value in their **attention**. Simply removing the [CLS] embedding from the ViT causes the *softmax* to sum to 1 over all image patches, which may yield a misleading interpretation that there *is* always a change even for no-change pairs, as it generates nonzero attention values.

Since the [CLS] pays more attention to class-specific tokens [13], another approach to improve the scalability of ViTs is to identify the most important tokens based on their attention value to the [CLS] token [24, 33]. The tokens with small attention values can be removed to reduce the computations further. Yet, in this work, we drop the image patches and directly use the [CLS] to bottleneck the final representation for both **localization** and **captioning** tasks.

**Concept bottleneck models** (CBMs) [17, 28, 30, 36, 48, 61] are a class of self-interpretable classifiers that map the input image to a set of human-predefined features (a.k.a. “concepts”), which are then used to derive model predictions. That is, CBMs offer a bottleneck that linearly combines the pre-defined features. In contrast, TAB offers a bottleneck for attention over patch embeddings. These two approaches are orthogonal and can be used together.

**Model editing** enables users to change a certain parameter of a machine learning model at test time for intervention or reprogramming [40]. These efforts ranged from editing facts in language models [40, 41], to textual descriptors in image classifiers [48] or neurons in classifiers and generative models [8, 9]. Our work is the first to explore editing the **attention** of the vision encoder of a VLM.

**Change captioning** Most CC models often rely on MHSA to extract image features and to compare two images [23, 47, 64]. However, their ViTs often contain many layers and attention heads, posing a challenge to feature attribution and intervention. In contrast, we take the VLM architecture by [23] designed for CC and **simplify** it by converting the last cross-attention layer (inside the vision encoder) into a

<sup>1</sup>Code and data are available on [GitHub](#).

TAB (Fig. 2), which results in (1) improved **captioning** accuracy; (2) superior change **localization** via attention; and (3) **editability** for users.

Furthermore, most CC research trained a VLM to caption changes directly without explicitly teaching it how to localize changes [23, 47, 58, 64]. In contrast, we supervise VLMs (via TAB) with localization annotations, yielding improved captions and change **localization** capability.

### 3. Method

#### 3.1. Architecture

To demonstrate TAB for VLMs, we take CLIP4IDC architecture [23], a SotA CC model, and simplify its last cross-attention (MHSA [59]) layer into a TAB (Fig. 2a) and re-train this modified architecture (TAB4IDC) for captioning. Specifically, below are the architectural changes we make:

1. Replacing cross-attention by co-attention [38] (Fig. 2c).
2. Reducing the number of heads from 12 to 1.
3. Removing the initial skip connection (Fig. 2b).
4. Adding a dynamic attention gating mechanism that zeroes out the [CLS] attention when the total attention over image patches is zero (Fig. 2c).

TAB4IDC first extracts visual features from the two images and then localizes changes (if any) using TAB (Fig. 2a). Then, it passes the [CLS] embedding of each image to a language model (LM), which outputs a caption that either states that no changes are detected or what the changes are.

**Vision encoder** Following CLIP4IDC, we use the initial convolution layer in CLIP’s ViT [52] (for both B/16 and B/32) to patchify each image  $I_1$  and  $I_2$  into  $n$  patches  $\in \mathbb{R}^d$ :

$$I_1 = \{p_{\text{cls}}^1, p_1^1, \dots, p_n^1\} + pos \quad (1)$$

$$I_2 = \{p_{\text{cls}}^2, p_1^2, \dots, p_n^2\} + pos \quad (2)$$

where  $p_{\text{cls}}$  and  $p_i$  represent the [CLS] and patch tokens of each image, respectively and  $pos \in \mathbb{R}^{(n+1) \times d}$  is the positional embedding. Each token is expressed by an embedding vector of size  $d = 768$  after the convolution layer. Next, we use a 9-layer, 12-head MHSA Transformer encoder ( $F$ ) to extract features from each single image (Fig. 2a).

Then, we concatenate the patch embeddings from two images and pass them to a 2-layer, 12-head ViT ( $F'$ ), akin to CrossViT [15], to enable **image comparison**:

$$y = F'(\{F(I_1) + e_1, F(I_2) + e_2\} + pos') \quad (3)$$

We use a learnable joint positional embedding,  $pos' \in \mathbb{R}^{2(n+1) \times d}$ , which lets the model represent the position of each patch in the input images. Following CLIP4IDC [23] and CrossViT [15], we use a pair of extra learnable positional embeddings,  $e_1$  and  $e_2 \in \mathbb{R}^d$ , to represent the order of each image in the pair.

$y$  from Eq. (3) can be seen as  $y = [f^1 \parallel f^2]$  (Fig. 2b), where  $f^1, f^2 \in \mathbb{R}^{(n+1) \times d}$  are the contextualized embeddings of the first and second image after  $F'$ , and  $[\parallel]$  is the concatenation operation.

**Bottleneck** We take the vanilla MSHA layer [59] and simplify it by restricting its information flow through the co-attention [38] mechanism for our attention bottleneck.

The co-attention [38], given the intermediate contextualized embeddings  $f^1$  and  $f^2$  from each image, obtains  $Q$ ,  $K$ , and  $V$  as in the vanilla Transformer layer [59]. Yet,  $K$  and  $V$  are swapped between the attention branches of  $f^1$  and  $f^2$  (Fig. 2c). That is, the co-attention produces two embeddings,  $H(f^1, f^2)$  and  $H(f^2, f^1)$  via:

$$Q = W^q f^q, \quad K = W^k f^k, \quad V = W^k f^k \quad (4)$$

$$A = \text{softmax}\left(\frac{QK^T}{\sqrt{d_k}}\right) \quad (5)$$

$$A' = A_{\text{cls}} \times \sum_{i=1}^n A_{\text{cls},i} \quad (6)$$

$$H^q(f^q, f^k) = W^o A' V \quad (7)$$

where  $W^q$ ,  $W^k$ , and  $W^o$  are learnable weights.  $A_{\text{cls},i}$  is the attention value between the [CLS] row in the  $Q$  matrix and the  $i$ -th patch row in the  $K$  matrix.

For intervention and interpretability, we reduce the number of heads from 12 to 1, yielding only one attention map (Eq. (5)) per image (Fig. 2d). We then remove the first skip connection in the Transformer layer to block any information leak in the flow (Fig. 2b). Finally, we mask all the tokens in the attention map, except the [CLS]. This yields  $H_{\text{cls}}^1, H_{\text{cls}}^2 \in \mathbb{R}^d$  as the final image representations obtained in TAB (Fig. 2c). We then apply a linear projection to map them to  $P^1, P^2 \in \mathbb{R}^{512}$ .

**Caption generation** Like CLIP4IDC [23], we use a 6-layer, encoder-decoder LM that translates the outputs of the vision encoder into a caption. Specifically, we pass  $P^1$  and  $P^2$  to a 3-layer, 8-head language encoder to generate intermediate representations, which are then decoded into a caption via a 3-layer, 8-head decoder (see [code](#) and [configuration](#)).

#### 3.2. Training

Like CLIP4IDC [23], our training has two stages: (1) adaptation and (2) captioning. Stage 1 aims to align the visual representations of two images to their change caption in the text space via CLIP’s contrastive loss [52]. This pre-trained vision encoder from Stage 1 then serves as an initialization for Stage 2, where both the vision encoder and the LM are trained with a next-token prediction and an attention loss.

##### 3.2.1 Stage 1: Adaptation

We use a retrieval loss function [23] to adapt the visual representations in Stage 1:

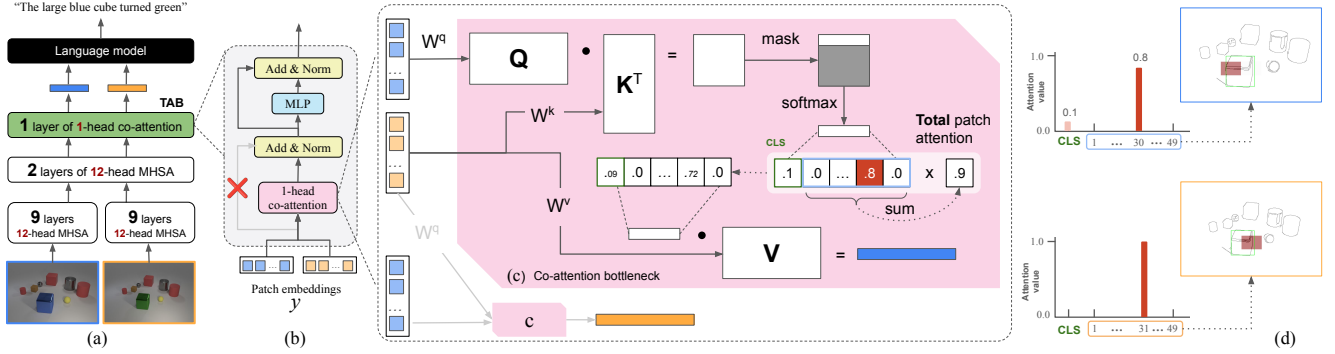


Figure 2. We insert an attention bottleneck (TAB) into a VLM architecture and train it to perform change **captioning** (a). TAB is a 1-head co-attention [38] Transformer layer (b) that has a skip connection removed  $\textcolor{red}{X}$  so that the 1-head attention (c) serves as an information bottleneck, akin to the forget gate in LSTM, directly controls the visual information that flows into the language model. The attention maps in TAB show precisely how much each patch contributes to the VLM response (d).

$$\mathcal{L}_{i2t} = \frac{-1}{B} \sum_i^B \log \frac{\exp(s(v_i, g_i)/\tau)}{\sum_{j=1}^B \exp(s(v_i, g_j)/\tau)} \quad (8)$$

$$\mathcal{L}_{t2i} = \frac{-1}{B} \sum_i^B \log \frac{\exp(s(v_i, g_i)/\tau)}{\sum_{j=1}^B \exp(s(v_j, g_i)/\tau)} \quad (9)$$

$$\mathcal{L}_{\text{Stage1}} = \mathcal{L}_{i2t} + \mathcal{L}_{t2i} \quad (10)$$

where  $\mathcal{L}_{i2t}$  and  $\mathcal{L}_{t2i}$  are the loss functions of image pair-to-text and text-to-image pair retrieval, respectively.  $v_i$  is the mean pooling of  $P^1$  and  $P^2$ ; and  $g_i$  is the textual embeddings extracted from the caption using CLIP [52] text encoder for  $i$ -th image-text pair.

### 3.2.2 Stage 2: Captioning

Stage 2 training has two losses:  $\mathcal{L}_{\text{Stage2}} = \mathcal{L}_{CE} + \mathcal{L}_{att}$ .

Like [23], we supervise VLMs to generate a caption given two images using a Cross Entropy (CE) loss over the next word (see App. A).

In addition to a captioning CE loss, we also use an **attention supervision** loss ( $\mathcal{L}_{att}$ ) to encourage TAB to focus on relevant image patches. We derive a groundtruth attention map  $G \in [0, 1]^n$  from a human-annotated bounding box  $b$  (available in CLEVR-Change and OpenImages-I) by assigning 1 to the patch that has the largest intersection with  $b$  and 0 to all other  $n - 1$  patches. That is, when there is no change, the attention value should be 1 for the [CLS] embedding and 0 for all  $n$  patch embeddings.

Our attention loss would minimize the cosine distance between the groundtruth attention map  $G$  and the attention map  $A_{cls} \in [0, 1]^n$  in TAB:

$$\mathcal{L}_{att} = 1 - \frac{\langle A_{cls}, G \rangle}{\|A_{cls}\| \cdot \|G\|} \quad (11)$$

## 4. Evaluation

### 4.1. Datasets

We train and evaluate TAB4IDC’s **captioning** and TAB’s **localization** capabilities on three distinct CC datasets that vary in the number of changes, types of changes, difficulty levels, and types of images (Tab. 1).

**CLEVR-Change** [47] contains  $\sim 80K$  image pairs where 40K contain exactly one change (change) and the other 40K has no changes (no-change). Images contain primitive 3D shapes and are rendered using Blender [18].

**OpenImages-I** [43] consists of  $\sim 2.5M$  pairs of images ( $\sim 1.28M$  for each change and no-change) where one object is removed. In each change pair, one image is taken from OpenImages [31] and the other is a clone but has one object removed by the LaMa inpainter [57] based on its human-annotated bounding box. Following Nguyen et al. [43], we apply random rotation and zoom to a random image in each pair to create viewpoint differences. We use the object-name annotations of OpenImages and follow Park et al. [47] to create change captions using predefined templates (see App. C).

**Spot-the-Diff (STD)** [27] has  $\sim 13K$  image pairs captured from CCTV videos in VIRAT Video dataset [45]. Each image pair contains more than one change and is captioned by humans. For **localization** evaluation, we add a no-change class (1K pairs of identical images) to the test set, which initially contains 1K pairs of changed images.

### 4.2. Metrics

**Change captioning** Following [23, 47], we use five metrics for evaluating the n-grams of generated captions: BLEU-4 [46], METEOR [6], ROUGE-L [34], and CIDEr [60]. For a semantics assessment, we also use BERTScore [22, 67] to evaluate the meanings of captions.

**Attention map visualization** The attention bottleneck

Table 1. We conduct experiments on three distinct change **captioning** datasets of varying image sources, numbers of changes, and difficulties.

Dataset	Number of pairs	Image type	Change type	# Changes	No-change	Annotations
 [47]	79,606	3D-rendered	Color, Material Add, Remove, Move	1	✓	caption bounding box
 [43]	2,559,918	real-world	Add, Remove	1	✓	caption bounding box name of changed objects
 [27]	13,192	real-world	Add, Remove, Move	$\in [1\dots 7]$	✗	caption
 [53]	60,000	real-world	Add, Remove	$\in [1\dots 24]$	✗	bounding box

in TAB4IDC attends to the change locations in the attention map (Eq. (5)) and, therefore, acts as a change detector. To evaluate TAB’s **localization** performance, we derive heatmaps from  $A_{cls}$ , *i.e.*, the [CLS] row in the attention map (Eq. (5)) in each branch of the co-attention (see Fig. 2c). This row contains exactly  $n + 1$  attention values per image ( $n = 49$  and 196 in B/32 and B/16, respectively). We drop the [CLS] attention value ( $A_{cls,cls}$ ) and keep the  $n$  attention values of the image patches (see Fig. 2d), *i.e.*, the  $A_{cls,i}$  values where  $i \in [1\dots n]$ .

We reshape the vector  $A_{cls,i}$  of size  $n \in \{49, 196\}$  to a square matrix of size  $7 \times 7$  and  $14 \times 14$  for B/32 and B/16, respectively. Then, we upscale the reshaped  $A_{cls,i}$  to the input image size via the nearest-neighbor interpolation (see Fig. 11) for TAB and the CC baselines [23, 47, 51] to obtain the final heatmaps. Compared to attention visualization methods in CC baselines [23, 47] that use cubic interpolation (see Fig. 10), our nearest-neighbor approach better shows the actual values of the attention map per patch (Fig. 3; 1b vs. 1c), and yields fewer nonzero pixels on no-change (see Fig. 3; 2b vs. 2c).

**Change localization** In this task, we aim to approximate the accuracy of the attention map in highlighting the image patches that contribute to the predicted captions in change and no-change pairs. A common approach to attention map evaluation is using the *object localization* techniques [5, 7, 66, 68]. However, these metrics, such as pointing game accuracy (PG) [66], evaluate the attention maps by localizing a target object present in an image [5, 7, 68]. That is, for change **localization**, they evaluate the attention maps only for change pairs that contain a groundtruth changed object. The attention map should not highlight any objects in no-change pairs, as there are no changes across the images.

Here, we introduce **pointing game<sup>+</sup> accuracy (PG<sup>+</sup>)** to measure the localization accuracy for both change and no-change pairs. Similar to [5, 12, 21], we derive multiple bounding boxes from the attention map, which is reshaped to the input image size, by thresholding it at different  $t \in [0.0 : 0.05 : 0.95]$  values. At each  $t$  value, for change pairs, accuracy is the frequency of when a derived bounding

box intersects with the groundtruth box, and for no-change pairs, accuracy is when the attention map is all zero after the thresholding (see Fig. 3-2d). We choose the best  $t$  value that yields the best mean accuracy over change and no-change pairs on the validation sets.

**Effects of visualization on localization accuracy** Since the visualization method in CC baselines [23, 47, 51], always yields an attention map with at least one peak even for no-change pairs (see Fig. 3-2b), their original localization is poor (see Tab. 2). However, our proposed thresholding and interpolation method (Fig. 11) improves the baseline methods [23, 47, 51] **localization** accuracy (see Tab. 2), specifically on no-change pairs.

**Attention Editing** A caption in change captioning must include two main pieces of information: (1) Is there a change across two images? (2) If there is a change, which object? Therefore, we measure how **editing** the attention values in TAB affect these two pieces of information in the generated caption via:

- **Change and no-change accuracy:** We evaluate the correctness of the captions by comparing their template to the groundtruth caption templates (see App. C). The evaluation is based on exact word matching, and we report the model’s accuracy in expressing whether a change has occurred or not.
- **Object accuracy:** Change pairs in  are created by inpainting a single object [43], for which we can access the groundtruth object name. Since a major error in TAB4IDC captions is predicting a wrong object name, we measure the object accuracy before and after editing the attention values by (1) extracting the object name from the predicted caption using the templates (see App. C), and (2) applying exact word matching w.r.t groundtruth object name.

## 5. Results

### 5.1. TAB4IDC outperforms other Transformer-based baselines in change captioning

By design, TAB reduces the capacity of the vision encoder, which may limit the VLM’s captioning performance.

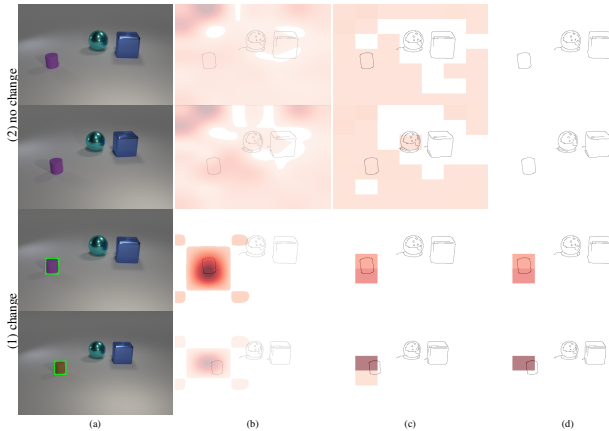


Figure 3. For each input pair in (a), the interpolation method in CLIP4IDC [23] (see Fig. 10) yields many nonzero attention values for no-change pairs (2b). In our visualization, we use the nearest-neighbor method (Fig. 11) that leads to fewer nonzero values on no-change (2c). For baseline methods, the thresholding substantially improves the attention map’s quality for no-change pairs (2d), where there is no target object for detection.

Table 2. The common interpolation method used for upscaling the attention map leads to low PG<sup>+</sup> accuracy (0.0%) on (b), here for CLIP4IDC [23]. We use the nearest neighbor approach (Fig. 11) and, then, threshold the attention map at different values to find the most important patches based on their values. This improves the baseline method’s overall PG<sup>+</sup> (90.15%).

Method	ViT	Interpolation	Thresh.	Change	No-change	Mean
Baseline	B/32	cubic	✗	79.98	0.0	39.99
Ours	B/32	nearest neighbor	✓	84.10	96.21	<b>90.15</b>

Therefore, after building a TAB bottleneck in the baseline VLM (CLIP4IDC) and training it, we test how our model (TAB4IDC) performs in **captioning** compared to CLIP4IDC and other VLMs in the supervised learning setting.

**Experiment** Following [47, 64], we train our model on CLEVR-Change (b) and compare it to CLIP4IDC [23], DUDA [47], MCCFormer [51] and IDC-PCL [64]. We also train and test our models on the real-world images in OpenImages-I (c) and the camera surveillance dataset of STD (d). We reproduce the results of DUDA, MCCFormers, and CLIP4IDC using their public code bases [1–3].

**Results** At the higher-resolution attention maps, *i.e.*, smaller patch sizes of B/16, TAB4IDC consistently outperforms the counterpart model of the CLIP4IDC [23]. This suggests that **the bottleneck does not limit the information flowing into the LM**. Furthermore, our proposed training regime with attention supervision improves the **captioning** accuracy (+1.5 vs. +1.1 on (c); Tab. 4), compared to the baseline.

With low-res attention (ViT-B/32), TAB4IDC performs

Table 3. **Captioning** (b): TAB4IDC performs better than CC methods that use RNN attention, DUDA [47], and the models that combine CNN and Transformers [51]. Compared to pure Transformer-based VLMs, TAB4IDC is far better than IDC-PCL and on par with its predecessor, CLIP4IDC.

Method	ViT	<b>B-4</b>	<b>M</b>	<b>R</b>	<b>C</b>	<b>BERTScore</b>
DUDA [47]		✗	47.3	33.9	n/a	112.3 67.4
MCCFormer-D [51]		✗	52.4	38.3	n/a	121.6 n/a
MCCFormer-S [51]		✗	57.4	41.2	n/a	125.5 n/a
IDC-PCL [64]		✗	51.2	36.2	71.7	128.9 n/a
CLIP4IDC [23]	B/32	56.9	38.4	76.4	150.7	74.3
CLIP4IDC [23]	B/16	52.9	38.7	76.4	144.7	74.2
TAB4IDC	B/32	55.5	38.0	76.3	149.6	73.7 <b>(-0.6)</b>
TAB4IDC	B/16	56.4	38.6	<b>77.7</b>	<b>153.0</b>	<b>75.8</b> <b>(+1.6)</b>

Table 4. **Captioning** (c): Our proposed TAB4IDC performs better than CLIP4IDC on captioning changes across natural images. The attention supervision in TAB improves the captioning accuracy in TAB4IDC (+0.4 in BERTScore).

Method	ViT	Attn. Sup.	<b>B-4</b>	<b>M</b>	<b>R</b>	<b>C</b>	<b>BERTScore</b>
CLIP4IDC [23]	B/32	✗	82.8	56.0	93.6	296.5	92.4
CLIP4IDC [23]	B/16	✗	87.5	60.3	95.6	328.7	95.1
TAB4IDC	B/32	✓	91.4	62.1	94.7	302.0	93.8 <b>(+1.4)</b>
TAB4IDC	B/16	✓	<b>92.4</b>	<b>64.5</b>	<b>96.9</b>	<b>335.6</b>	<b>96.6</b> <b>(+1.5)</b>
TAB4IDC	B/16	✗	91.9	63.8	96.6	324.4	96.2 <b>(+1.1)</b>

Table 5. **Captioning** (d): TAB4IDC with no attention supervision, requires more patches (the higher-resolution ViT-B/16) to be on par with CLIP4IDC.

Method	ViT	<b>B-4</b>	<b>M</b>	<b>R</b>	<b>C</b>	<b>BERTScore</b>
CLIP4IDC [23]	B/32	11.6	14.2	35.0	47.4	<b>29.4</b>
CLIP4IDC [23]	B/16	10.0	12.7	32.6	47.6	23.0
TAB4IDC	B/32	11.0	13.5	33.0	37.7	22.6 <b>(-6.8)</b>
TAB4IDC	B/16	11.2	13.5	33.0	<b>51.3</b>	28.3 <b>(+5.3)</b>

on par with its baseline (-0.6 on (b), +1.4 on (c); Tabs. 3 and 4). Our model is the SotA on (b) and (c) perhaps because the training set is large and the groundtruth boxes are available to supervise the attention maps.

The largest difference is on (d)—TAB4IDC outperforms CLIP4IDC at high-res attention (+5.3 in B/16; Tab. 5) but underperforms at low resolution (-6.8 in B/32; Tab. 5). An explanation is that there are no groundtruth bounding boxes in (d), so no attention supervision is applied. Furthermore, the image pairs in (d) often contain many small changes, which benefit from high-res attention.

## 5.2. TAB outperforms MHSA layers and RNN-based attention in change localization

We aim to test how well TAB attention communicates the information (1) that no change is detected (no-change cases); and (2) of the location of the changed object in

Table 6. **Localization** : Under  $PG^+$ , TAB localizes changes far better than the attention maps of CC baselines. TAB uses only 1 head compared to the 12-head attention in CLIP4IDC [23] and prior models.

Method	ViT	Change	No-change	Mean
DUDA [47]		68.51	94.20	81.36
MCCFormer-D [51]		78.85	0.00	39.42
MCCFormer-S [51]		72.96	0.61	36.78
CLIP4IDC [23]	B/32	84.10	96.21	90.15
CLIP4IDC [23]	B/16	77.37	91.56	84.47
TAB	B/32	91.59	98.66	95.13 (
TAB	B/16	94.00	99.50	

change cases.

**Experiment** We take the VLM trained in Sec. 5.1 and conduct an object **localization** experiment on its TAB to evaluate the  $PG^+$  accuracy across three datasets (, , and ). We compare its accuracy to CC methods with **localization** ability. We hypothesize that given the attention supervision during training, TAB should yield a more precise attention map for each predicted caption.

**Results** Across different attention map resolutions (ViT-B/16 and B/32) and three datasets (, and ), TAB consistently localizes *object-level* differences better than the MHSA layer in CLIP4IDC. That is, **our proposed 1-head co-attention Transformer bottleneck yields attention maps that outperform baselines in communicating the predicted caption for both change and no-change pairs** (see Figs. 4 and 5). Perhaps, the reason is our proposed attention supervision during VLM training, where the attention map in TAB is forced to match the groundtruth attention ( vs. on ; Tab. 7 and Fig. 8).

TAB, using the high-res attention (ViT-B/16), has the largest delta with its MHSA counterpart in CLIP4IDC ( vs. on , vs. on ; Tabs. 6 and 7), compared to the low-res attention (ViT-B/32). The smaller patches in ViT-B/16, which help point to small objects in and , are perhaps the main reason for this delta. On , we use PG for evaluation because it only includes change pairs, where TAB is SotA change detector, and outperforms CLIP4IDC by (53.5 vs. 49.55%). This suggests that the attention map in TAB more frequently attends to image patches that contain the changed object, even without attention supervision.

### 5.3. Intervening by assigning more accurate attention in TAB yields improved VLM captions

Our attention bottleneck in TAB4IDC successfully performs localization in both change and no-change cases. Furthermore, the overall strong **localization** ability of the attention is observed together with the VLM’s **captioning** performance. Here, we aim to test if the attention values in

Table 7. **Localization** : TAB substantially outperforms MHSA layers in CLIP4IDC [23] on change localization under  $PG^+$ . The high-res backbone (B/16) performs better than the low-res (B/32) as most objects in are small. Our proposed attention supervision also improves the **localization** performance, especially across change pairs (32.24 vs. 98.40).

Method	ViT	Attn. Sup.	Change	No-change	Mean
CLIP4IDC [23]	B/32		24.55	83.74	54.14
CLIP4IDC [23]	B/16		6.12	99.85	52.98
TAB	B/32		99.56	96.66	98.11 (
TAB	B/16		98.40	99.98	
TAB	B/16		32.24	91.23	61.73 (

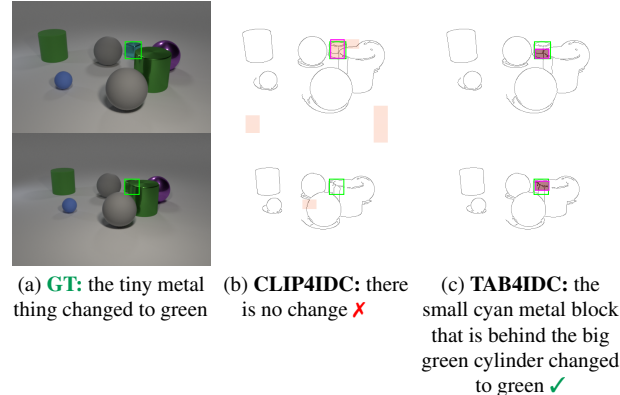


Figure 4. Compared to MHSA layer in CLIP4IDC (b) TAB better localizes the changed object that contributes to the predicted caption (c), for quantitative results we evaluate  $PG^+$  against the groundtruth () in .

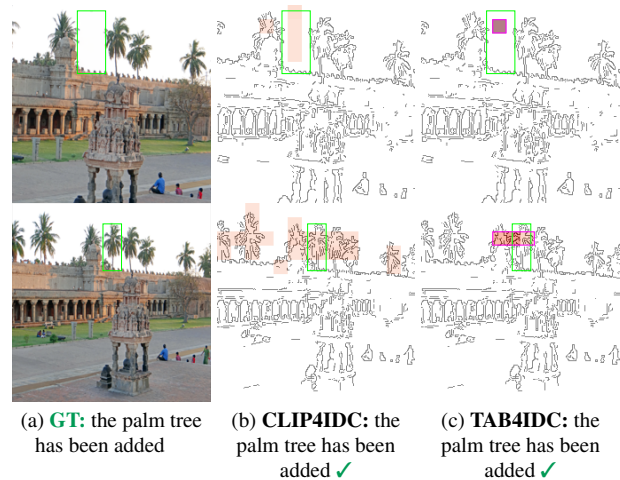


Figure 5. On , the MHSA attention of CLIP4IDC [23] often highlights many patches corresponding to the class name (here, palm tree) in the input image (b). In contrast, TAB points at exactly the only one palm tree that is changed.

TAB have a cause-and-effect relationship with the captions by TAB4IDC. We conduct two *editing* experiments: (1) CORRECTATTENTION, where the user replaces the attention map with groundtruth attention for wrong predictions. We expect that the correct attention maps improve *captioning* performance. (2) ZEROATTENTION, where the attention map is replaced with an all-zero map, and we desire that model captions any input as a no-change.

**Experiment** We use the groundtruth annotations ( $G$ ) of  and  that we used in Eq. (11) to conduct the debugging experiment during inference. Specifically, (1) for those image pairs that the predicted caption is wrong, we replace the attention map ( $A_{cls}$  in Eq. (5)) with  $G$ , and (2) for all the pairs, we replace  $A_{cls}$  with an all-zero vector and make  $A_{cls,cls} = 1$ . Finally, we evaluate the *editing* based on the common errors in the original captions.

**Results** In CORRECTATTENTION, replacing the attention map with groundtruth helps VLM to predict captions that match the groundtruth caption more frequently (see Figs. 1, 6 and 7). Similarly, in ZEROATTENTION, replacing the original attention map with an all-zero map, causes the VLM to predict a no-change caption for the input pair regardless of the groundtruth class (App. F.3). On image pairs, where the original predicted caption is wrong, TAB provides an interface during inference to debug the model by correcting its attention values. Furthermore, **TAB, when trained both with and without attention supervision, allows user interventions during test time** (see Tab. 8 a and c). This suggests that our proposed 1-head attention mechanism in TAB acts as a switch, which turns off the image patches for no-change pairs and turns them on for change pairs.

Specifically, CORRECTATTENTION improves the change and no-change accuracy on both  and  (99.93% to 100% on Tab. 8a; 94.30% to 100.0% Tab. 8b). This is because TAB predicts the caption based on the attention values of the image patches. ZEROATTENTION, conversely, only improves the no-change accuracy since the new attention values are only correct for no-change. Moreover, the change detection property of the attention maps in TAB, contributes to the object accuracy. When the attention values point to the changed object the, the object accuracy in predicted captions increases (88.92% to 91.49%; Tab. 8a).

#### 5.4. TAB, compared to the MHSA layers in VLM captioners, is a better zero-shot change locator

We use the VLMs trained for CC on  , which contain only one change, and aim to evaluate if the MHSA layer in CLIP4IDC [23] and TAB in TAB4IDC can localize multiple changes in an unseen dataset ( ) without further training.

**Experiment** We include a SotA change detection (CD)

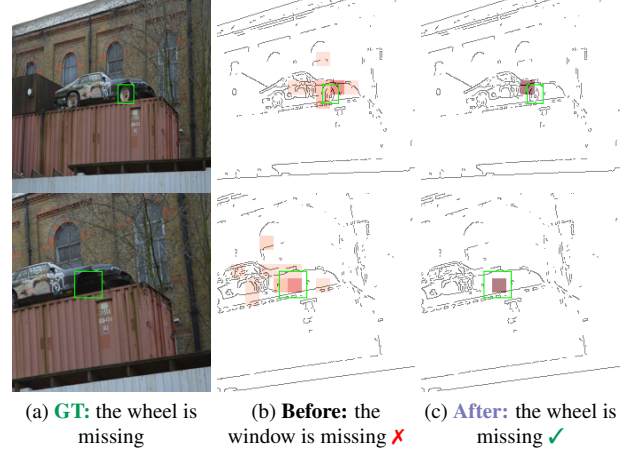


Figure 6. The attention maps from TAB on  , is an interface to debug the model by pointing to the correct patches in the input image (a) so that the predicted caption describes the changed object (c).

Table 8. **Editing**  : On  and  , ZEROATTENTION fools the model to classify all the input pairs as no-change pairs (0% and 100% accuracy over change and no-change, respectively). CORRECTATTENTION, in contrast, helps the model to predict the correct pair type more often. Correcting the attention values also helps (+2.57) and (+2.32) in predicting the correct object name in  .

Dataset	Sup.	Attention 	Acc. Change		Acc. No-change		Acc. object name	
			base		base		base	
a 	✓	ZERO	99.93	0.0 ✓	100.0	100.0 ✓	88.92	0.0 ✓
		CORRECT ↑	99.93	100.0 ✓	100.0	100.0 ✓	88.92	91.49 ✓
b 	✓	ZERO	94.30	0.0 ✓	99.42	100.0 ✓	-	-
		CORRECT ↑	94.30	100.0 ✓	99.42	100.0 ✓	-	-
c 	✗	ZERO	97.62	0.0 ✓	100.0	100.0 ✓	86.86	0.0 ✓
		CORRECT ↑	97.62	99.83 ✓	100.0	100.0 ✓	86.86	91.24 ✓

method, CYWS [53], as an upper bound, and report the PG<sup>+</sup> on  as a baseline accuracy for CYWS, TAB4IDC and CLIP4IDC [23]. CYWS [53] is a U-Net-based CD framework trained on COCO-Inpainted  , using the bounding box supervision. We consider CYWS [53] an upper bound accuracy because it is trained on real-world image pairs with multiple changes ( ) similar to  .

**Results** Overall, TAB outperforms the MHSA layer of CLIP4IDC [23] by  $\sim$ +44 points in mean PG<sup>+</sup> (Tab. 9). The main reason is TAB’s better performance on no-change pairs. On average, TAB and the MHSA layer are worse than CYWS [53] because they use the attention values (softmax output) to localize multiple changes in  . We hypothesize that the large gap is due to attention values spreading over many changes (see Fig. 12), which causes them not to pass the heatmap discretization in PG<sup>+</sup>. On  , TAB consistently outperforms CYWS [53] (99.19 vs. 89.76%). Com-

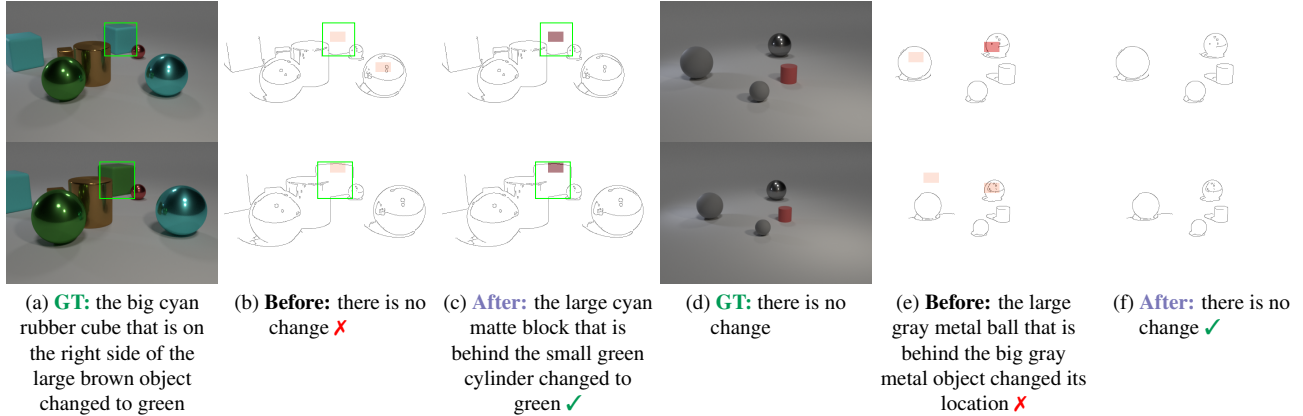


Figure 7. **Editing B/16 on** : Given input pairs of image (a, d), users can edit the original attention maps (b, e) by pointing to the correct patch (c) or zeroing the activation value (f) in TAB to improve the captions.

Table 9. **Zero-shot localization**: TAB performs better in zero-shot change **localization** in than the MHSA layer in CLIP4IDC [23], which is trained on . TAB also has smaller delta with CYWS [53], the upper bound zero-shot **localization** accuracy on , than CLIP4IDC [23].

Method	Train	Thresh.	Change		No-change		Mean	
CYWS [53]		✗	100.0	99.91	0.0	0.0	50.0	49.95
CYWS [53]		✓	99.92	81.73	100.0	99.72	<b>99.96</b>	89.76
CLIP4IDC [23]		✓	74.9	24.55	12.6	83.74	43.75	54.14
TAB		✓	75.9	98.40	100.0	99.98	87.95 (+44.2)	<b>99.19</b>

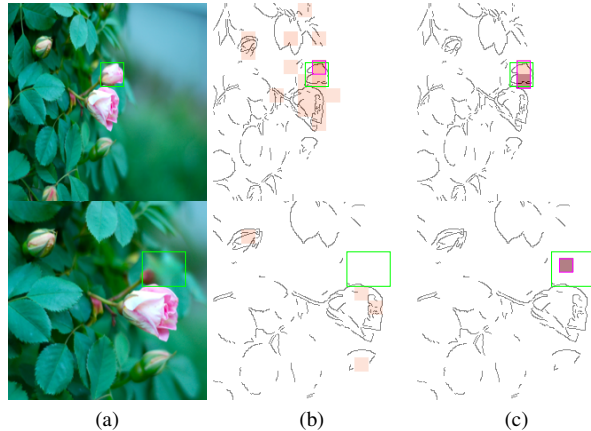


Figure 8. **Ablation**: TAB, without the Attention Supervision often only attends to the location that the object is present (b) in . The attention supervision mitigates this problem (c).

pared to the MHSA layer in CLIP4IDC [23], TAB improves the baseline accuracy of a CD method on .

## 6. Discussion and Conclusion

**Limitations** A limitation of TAB is its reliance on attention loss for accurate **localization** in change pairs. Moreover, the attention map in TAB requires more nonzero values over image patches for multi-change images, which makes the *softmax* function spread over more patches (*e.g.*, there are  $14 \times 14 = 196$  patches in ViT-B/16 compared to  $7 \times 7 = 49$  patches in ViT-B/32). This may cause TAB to have lower attention values over multi-change images. Another constraint is the size of the object that changed in different datasets. The smaller changes are in a dataset, the smaller patches TAB needs for more accurate **localization** and better **captioning** performance (Tab. 5).

We propose TAB, a self-explainable and editable bottleneck layer with a 1-head attention for CC. Our interactive interface allows users to intervene in decision-making, by which one can correct and audit VLMs’ decision. An intriguing future direction is to extend TAB to other core vision tasks, such as classification, image similarity comparison [49, 50], and image matching [62]. Given that TAB also improves the performance of our VLM change captioner, another valuable direction is to apply TAB to more general-purpose VLMs such as LLaVA [35]. Additionally, a VLM could be used to audit the attention values within TAB.

## Acknowledgment

We thank Peijie Chen, Thang Pham, Giang Nguyen, and Tin Nguyen at Auburn University for their feedback and discussions of the earlier results. AN was supported by the NSF Grant No. 1850117 & 2145767, and donations from NaphCare Foundation & Adobe Research.

## References

[1] GitHub - sushizixin/CLIP4IDC: CLIP4IDC: CLIP for Image Difference Captioning (AACL 2022) — [github.com/sushizixin/CLIP4IDC](https://github.com/sushizixin/CLIP4IDC). [Accessed 11-11-2022]. [6](#)

[2] GitHub - Seth-Park/RobustChangeCaptioning: Code and dataset release for Park et al., Robust Change Captioning (ICCV 2019) — [github.com/Seth-Park/RobustChangeCaptioning](https://github.com/Seth-Park/RobustChangeCaptioning). [Accessed 21-04-2023].

[3] GitHub - cvpaperchallenge/Describing-and-Localizing-Multiple-Change-with-Transformers — [github.com/cvpaperchallenge/Describing-and-Localizing-Multiple-Change-with-Transformers/](https://github.com/cvpaperchallenge/Describing-and-Localizing-Multiple-Change-with-Transformers/). [Accessed 26-11-2022]. [6](#)

[4] Samira Abnar and Willem Zuidema. Quantifying attention flow in transformers. *arXiv preprint arXiv:2005.00928*, 2020. [2](#)

[5] Chirag Agarwal and Anh Nguyen. Explaining image classifiers by removing input features using generative models. In *Proceedings of the Asian Conference on Computer Vision*, 2020. [5](#)

[6] Satanjeev Banerjee and Alon Lavie. METEOR: An automatic metric for MT evaluation with improved correlation with human judgments. In *Proceedings of the ACL Workshop on Intrinsic and Extrinsic Evaluation Measures for Machine Translation and/or Summarization*, pages 65–72, Ann Arbor, Michigan, 2005. Association for Computational Linguistics. [4](#)

[7] Naman Bansal, Chirag Agarwal, and Anh Nguyen. Sam: The sensitivity of attribution methods to hyperparameters. In *Proceedings of the ieee/cvf conference on computer vision and pattern recognition*, pages 8673–8683, 2020. [1, 2, 5](#)

[8] David Bau, Steven Liu, Tongzhou Wang, Jun-Yan Zhu, and Antonio Torralba. Rewriting a deep generative model. In *Computer Vision–ECCV 2020: 16th European Conference, Glasgow, UK, August 23–28, 2020, Proceedings, Part I 16*, pages 351–369. Springer, 2020. [2](#)

[9] David Bau, Jun-Yan Zhu, Hendrik Strobelt, Agata Lapedriza, Bolei Zhou, and Antonio Torralba. Understanding the role of individual units in a deep neural network. *Proceedings of the National Academy of Sciences*, 117(48):30071–30078, 2020. [2](#)

[10] Lucas Beyer, Xiaohua Zhai, and Alexander Kolesnikov. Better plain vit baselines for imagenet-1k. *arXiv preprint arXiv:2205.01580*, 2022. [2](#)

[11] Alexander Black, Jing Shi, Yifei Fan, Tu Bui, and John Collobosse. Vixen: Visual text comparison network for image difference captioning. In *Proceedings of the AAAI Conference on Artificial Intelligence*, pages 846–854, 2024. [2](#)

[12] Chunshui Cao, Xianming Liu, Yi Yang, Yinan Yu, Jiang Wang, Zilei Wang, Yongzhen Huang, Liang Wang, Chang Huang, Wei Xu, Deva Ramanan, and Thomas S. Huang. Look and think twice: Capturing top-down visual attention with feedback convolutional neural networks. In *2015 IEEE International Conference on Computer Vision (ICCV)*, pages 2956–2964, 2015. [5](#)

[13] Mathilde Caron, Hugo Touvron, Ishan Misra, Hervé Jégou, Julien Mairal, Piotr Bojanowski, and Armand Joulin. Emerging properties in self-supervised vision transformers. In *Proceedings of the IEEE/CVF international conference on computer vision*, pages 9650–9660, 2021. [2](#)

[14] Hila Chefer, Shir Gur, and Lior Wolf. Generic attention-model explainability for interpreting bi-modal and encoder-decoder transformers. In *Proceedings of the IEEE/CVF International Conference on Computer Vision (ICCV)*, pages 397–406, 2021. [1, 2](#)

[15] Chun-Fu Richard Chen, Quanfu Fan, and Rameswar Panda. Crossvit: Cross-attention multi-scale vision transformer for image classification. In *Proceedings of the IEEE/CVF international conference on computer vision*, pages 357–366, 2021. [3](#)

[16] Peijie Chen, Qi Li, Saad Biaz, Trung Bui, and Anh Nguyen. gscorecam: What objects is clip looking at? In *Proceedings of the Asian Conference on Computer Vision*, pages 1959–1975, 2022. [1, 2](#)

[17] Zhi Chen, Yijie Bei, and Cynthia Rudin. Concept whitening for interpretable image recognition. *Nature Machine Intelligence*, 2(12):772–782, 2020. [2](#)

[18] Blender Online Community. *Blender - a 3D modelling and rendering package*. Blender Foundation, Stichting Blender Foundation, Amsterdam, 2018. [4](#)

[19] Alexey Dosovitskiy, Lucas Beyer, Alexander Kolesnikov, Dirk Weissenborn, Xiaohua Zhai, Thomas Unterthiner, Mostafa Dehghani, Matthias Minderer, Georg Heigold, Sylvain Gelly, Jakob Uszkoreit, and Neil Houlsby. An image is worth 16x16 words: Transformers for image recognition at scale. In *International Conference on Learning Representations*, 2021. [1, 2](#)

[20] Roger Ferrod, Luigi Di Caro, and Dino Ienco. Towards a multimodal framework for remote sensing image change retrieval and captioning. *arXiv preprint arXiv:2406.13424*, 2024. [2](#)

[21] Ruth C Fong and Andrea Vedaldi. Interpretable explanations of black boxes by meaningful perturbation. In *Proceedings of the IEEE international conference on computer vision*, pages 3429–3437, 2017. [5](#)

[22] Yingqiang Ge, Wenyue Hua, Kai Mei, Juntao Tan, Shuyuan Xu, Zelong Li, Yongfeng Zhang, et al. Openagi: When llm meets domain experts. *Advances in Neural Information Processing Systems*, 36, 2024. [4](#)

[23] Zixin Guo, Tzu-Jui Wang, and Jorma Laaksonen. Clip4idc: Clip for image difference captioning. In *Proceedings of the 2nd Conference of the Asia-Pacific Chapter of the Association for Computational Linguistics and the 12th International Joint Conference on Natural Language Processing (Volume 2: Short Papers)*, pages 33–42, 2022. [2, 3, 4, 5, 6, 7, 8, 9, 13, 15](#)

[24] Joakim Bruslund Haurum, Sergio Escalera, Graham W Taylor, and Thomas B Moeslund. Which tokens to use? investigating token reduction in vision transformers. In *Proceedings of the IEEE/CVF International Conference on Computer Vision*, pages 773–783, 2023. [2](#)

[25] Genc Hoxha, Seloua Chouaf, Farid Melgani, and Youcef Smara. Change captioning: A new paradigm for multitemporal remote sensing image analysis. *IEEE Transactions on Geoscience and Remote Sensing*, 60:1–14, 2022. 2

[26] Xinyue Hu, Lin Gu, Qiyuan An, Mengliang Zhang, Liangchen Liu, Kazuma Kobayashi, Tatsuya Harada, Ronald M. Summers, and Yingying Zhu. Expert knowledge-aware image difference graph representation learning for difference-aware medical visual question answering. In *Proceedings of the 29th ACM SIGKDD Conference on Knowledge Discovery and Data Mining*, page 4156–4165, New York, NY, USA, 2023. Association for Computing Machinery. 2

[27] Harsh Jhamtani and Taylor Berg-Kirkpatrick. Learning to describe differences between pairs of similar images. In *Proceedings of the 2018 Conference on Empirical Methods in Natural Language Processing*, pages 4024–4034, 2018. 2, 4, 5

[28] Dmitry Kazhdan, Botty Dimanov, Mateja Jamnik, Pietro Liò, and Adrian Weller. Now you see me (cme): concept-based model extraction. *arXiv preprint arXiv:2010.13233*, 2020. 2

[29] Wonjae Kim, Bokyung Son, and Ildoo Kim. Vilt: Vision-and-language transformer without convolution or region supervision. In *International conference on machine learning*, pages 5583–5594. PMLR, 2021. 2

[30] Pang Wei Koh, Thao Nguyen, Yew Siang Tang, Stephen Mussmann, Emma Pierson, Been Kim, and Percy Liang. Concept bottleneck models. In *Proceedings of the 37th International Conference on Machine Learning*, pages 5338–5348. PMLR, 2020. 2

[31] Alina Kuznetsova, Hassan Rom, Neil Alldrin, Jasper R. R. Uijlings, Ivan Krasin, Jordi Pont-Tuset, Shahab Kamali, Stefan Popov, Matteo Malloci, Tom Duerig, and Vittorio Ferrari. The open images dataset V4: unified image classification, object detection, and visual relationship detection at scale. *CoRR*, abs/1811.00982, 2018. 4

[32] Mingjie Li, Bingqian Lin, Zicong Chen, Haokun Lin, Xianan Liang, and Xiaojun Chang. Dynamic graph enhanced contrastive learning for chest x-ray report generation. In *Proceedings of the IEEE/CVF Conference on Computer Vision and Pattern Recognition*, pages 3334–3343, 2023. 2

[33] Y. Liang, C. Ge, Z. Tong, Y. Song, J., , and P. Xie. Not all patches are what you need: Expediting vision transformers via token reorganizations. *International Conference on Learning Representations (ICLR)*. 2

[34] Chin-Yew Lin. ROUGE: A package for automatic evaluation of summaries. In *Text Summarization Branches Out*, pages 74–81, Barcelona, Spain, 2004. Association for Computational Linguistics. 4

[35] Haotian Liu, Chunyuan Li, Yuheng Li, and Yong Jae Lee. Improved baselines with visual instruction tuning. In *Proceedings of the IEEE/CVF Conference on Computer Vision and Pattern Recognition*, pages 26296–26306, 2024. 9

[36] Max Losch, Mario Fritz, and Bernt Schiele. Interpretability beyond classification output: Semantic bottleneck networks. *arXiv preprint arXiv:1907.10882*, 2019. 2

[37] Ilya Loshchilov and Frank Hutter. SGDR: Stochastic gradient descent with warm restarts. In *International Conference on Learning Representations*, 2017. 14

[38] Jiasen Lu, Dhruv Batra, Devi Parikh, and Stefan Lee. Vilbert: Pretraining task-agnostic visiolinguistic representations for vision-and-language tasks. *Advances in neural information processing systems*, 32, 2019. 2, 3, 4

[39] Zilin Lu, Yutong Xie, Qingjie Zeng, Mengkang Lu, Qi Wu, and Yong Xia. Spot the difference: Difference visual question answering with residual alignment. In *International Conference on Medical Image Computing and Computer-Assisted Intervention*, pages 649–658. Springer, 2024. 2

[40] Kevin Meng, David Bau, Alex Andonian, and Yonatan Beilinkov. Locating and editing factual associations in gpt. *Advances in Neural Information Processing Systems*, 35: 17359–17372, 2022. 2

[41] Eric Mitchell, Charles Lin, Antoine Bosselut, Christopher D Manning, and Chelsea Finn. Memory-based model editing at scale. In *International Conference on Machine Learning*, pages 15817–15831. PMLR, 2022. 2

[42] Giang Nguyen, Daeyoung Kim, and Anh Nguyen. The effectiveness of feature attribution methods and its correlation with automatic evaluation scores. *Advances in Neural Information Processing Systems*, 34:26422–26436, 2021. 1, 2

[43] Hung Huy Nguyen, Pooyan Rahmazadehgervi, Long Mai, and Anh Totti Nguyen. Improving change detection by incorporating correspondence information. In *Proceedings of the IEEE/CVF Winter Conference on Applications of Computer Vision (WACV)*, 2025. 2, 4, 5, 16

[44] Mehdi Nourelihi, Lars Kotthoff, Peijie Chen, and Anh Nguyen. How explainable are adversarially-robust cnns? *arXiv preprint arXiv:2205.13042*, 2022. 2

[45] Sangmin Oh, Anthony Hoogs, Amitha Perera, Naresh Cuntoor, Chia-Chih Chen, Jong Taek Lee, Saurajit Mukherjee, J. K. Aggarwal, Hyungtae Lee, Larry Davis, Eran Swears, Xioyang Wang, Qiang Ji, Kishore Reddy, Mubarak Shah, Carl Vondrick, Hamed Pirsiavash, Deva Ramanan, Jenny Yuen, Antonio Torralba, Bi Song, Anesco Fong, Amit Roy-Chowdhury, and Mita Desai. A large-scale benchmark dataset for event recognition in surveillance video. In *CVPR 2011*, pages 3153–3160, 2011. 4

[46] Kishore Papineni, Salim Roukos, Todd Ward, and Wei-Jing Zhu. Bleu: a method for automatic evaluation of machine translation. In *Proceedings of the 40th Annual Meeting on Association for Computational Linguistics*, page 311–318, USA, 2002. Association for Computational Linguistics. 4

[47] Dong Huk Park, Trevor Darrell, and Anna Rohrbach. Robust change captioning. In *Proceedings of the IEEE/CVF International Conference on Computer Vision*, pages 4624–4633, 2019. 2, 3, 4, 5, 6, 7, 15, 16

[48] Thang Pham, Peijie Chen, Tin Nguyen, Seunghyun Yoon, Trung Bui, and Anh Nguyen. PEEB: Part-based image classifiers with an explainable and editable language bottleneck. In *Findings of the Association for Computational Linguistics: NAACL 2024*, pages 2018–2053, Mexico City, Mexico, 2024. Association for Computational Linguistics. 2

[49] Hai Phan and Anh Nguyen. Deepface-emd: Re-ranking using patch-wise earth mover’s distance improves out-of-

distribution face identification. In *Proceedings of the IEEE/CVF Conference on Computer Vision and Pattern Recognition*, pages 20259–20269, 2022. 9

[50] Hai Phan, Cindy X Le, Vu Le, Yihui He, Anh Nguyen, et al. Fast and interpretable face identification for out-of-distribution data using vision transformers. In *Proceedings of the IEEE/CVF Winter Conference on Applications of Computer Vision*, pages 6301–6311, 2024. 2, 9

[51] Yue Qiu, Shintaro Yamamoto, Kodai Nakashima, Ryota Suzuki, Kenji Iwata, Hirokatsu Kataoka, and Yutaka Satoh. Describing and localizing multiple changes with transformers. In *Proceedings of the IEEE/CVF International Conference on Computer Vision*, pages 1971–1980, 2021. 2, 5, 6, 7

[52] Alec Radford, Jong Wook Kim, Chris Hallacy, Aditya Ramesh, Gabriel Goh, Sandhini Agarwal, Girish Sastry, Amanda Askell, Pamela Mishkin, Jack Clark, et al. Learning transferable visual models from natural language supervision. In *International conference on machine learning*, pages 8748–8763. PMLR, 2021. 3, 4

[53] Ragav Sachdeva and Andrew Zisserman. The change you want to see. In *Proceedings of the IEEE/CVF Winter Conference on Applications of Computer Vision*, pages 3993–4002, 2023. 2, 5, 8, 9

[54] Wojciech Samek, Grégoire Montavon, Sebastian Luschkin, Christopher J Anders, and Klaus-Robert Müller. Explaining deep neural networks and beyond: A review of methods and applications. *Proceedings of the IEEE*, 109(3):247–278, 2021. 2

[55] Sanjay Subramanian, William Merrill, Trevor Darrell, Matt Gardner, Sameer Singh, and Anna Rohrbach. Reclip: A strong zero-shot baseline for referring expression comprehension. In *Proceedings of the 60th Annual Meeting of the Association for Computational Linguistics (Volume 1: Long Papers)*, pages 5198–5215, 2022. 2

[56] Yanjun Sun, Yue Qiu, Maria Khan, Fumiya Matsuzawa, and Kenji Iwata. The stvchrono dataset: Towards continuous change recognition in time. In *Proceedings of the IEEE/CVF Conference on Computer Vision and Pattern Recognition (CVPR)*, pages 14111–14120, 2024. 2

[57] Roman Suvorov, Elizaveta Logacheva, Anton Mashikhin, Anastasia Remizova, Arsenii Ashukha, Aleksei Silvestrov, Naejin Kong, Harshith Goka, Kiwoong Park, and Victor Lempitsky. Resolution-robust large mask inpainting with fourier convolutions. In *Proceedings of the IEEE conference on computer vision and pattern recognition*, 2021. 4

[58] Hao Tan, Franck Dernoncourt, Zhe Lin, Trung Bui, and Mohit Bansal. Expressing visual relationships via language. In *Proceedings of the 57th Annual Meeting of the Association for Computational Linguistics*, pages 1873–1883, 2019. 2, 3

[59] Ashish Vaswani, Noam Shazeer, Niki Parmar, Jakob Uszkoreit, Llion Jones, Aidan N Gomez, Łukasz Kaiser, and Illia Polosukhin. Attention is all you need. *Advances in neural information processing systems*, 30, 2017. 1, 2, 3

[60] Ramakrishna Vedantam, C Lawrence Zitnick, and Devi Parikh. Cider: Consensus-based image description evaluation. In *Proceedings of the IEEE conference on computer vision and pattern recognition*, pages 4566–4575, 2015. 4

[61] Bowen Wang, Liangzhi Li, Yuta Nakashima, and Hajime Nagahara. Learning bottleneck concepts in image classification. In *Proceedings of the ieee/cvf conference on computer vision and pattern recognition*, pages 10962–10971, 2023. 2

[62] Olivia Wiles, Sébastien Ehrhardt, and Andrew Zisserman. Co-attention for conditioned image matching. In *Proceedings of the IEEE/CVF conference on computer vision and pattern recognition*, pages 15920–15929, 2021. 9

[63] An Yan, Xin Wang, Tsu-Jui Fu, and William Yang Wang. L2C: Describing visual differences needs semantic understanding of individuals. In *Proceedings of the 16th Conference of the European Chapter of the Association for Computational Linguistics: Main Volume*, pages 2315–2320, Online, 2021. Association for Computational Linguistics. 2

[64] Linli Yao, Weiyang Wang, and Qin Jin. Image difference captioning with pre-training and contrastive learning. In *Proceedings of the AAAI Conference on Artificial Intelligence*, pages 3108–3116, 2022. 2, 3, 6

[65] Xiaohua Zhai, Alexander Kolesnikov, Neil Houlsby, and Lucas Beyer. Scaling vision transformers. In *Proceedings of the IEEE/CVF conference on computer vision and pattern recognition*, pages 12104–12113, 2022. 2

[66] Jianming Zhang, Sarah Adel Bargal, Zhe Lin, Jonathan Brandt, Xiaohui Shen, and Stan Sclaroff. Top-down neural attention by excitation backprop. *International Journal of Computer Vision*, 126(10):1084–1102, 2018. 5

[67] Tianyi Zhang, Varsha Kishore, Felix Wu, Kilian Q Weinberger, and Yoav Artzi. Bertscore: Evaluating text generation with bert. *arXiv preprint arXiv:1904.09675*, 2019. 4

[68] Bolei Zhou, Aditya Khosla, Agata Lapedriza, Aude Oliva, and Antonio Torralba. Learning deep features for discriminative localization. In *Proceedings of the IEEE conference on computer vision and pattern recognition*, pages 2921–2929, 2016. 5

# TAB: Transformer Attention Bottlenecks enable User Intervention and Debugging in Vision-Language Models

## Supplementary Material

### A. Implementation details

#### A.1. Framework

We adopt our CC framework from CLIP4IDC [23] (see Fig. 9). We resize the input images to  $224 \times 224$ . The images are then patchified into 49 patches for B/32 and 196 patches for B/16 using the first convolution layer in CLIP ViT-B/32 and ViT-B/16, respectively. The intermediate embedding dimension in the vision Transformers is  $d = 768$  and the final projected embedding is 512. We use the encoder-decoder language model to perform the next token prediction.

#### A.2. Training

We fix the first convolution layer and use the retrieval loss (Eq. (10)) to align vision and language blocks. We use the initial learning rate of  $10^{-7}$  and use a cosine scheduler with Adam optimizer. We continue the training in the alignment stage for 12 epochs (see Tab. 10). We drop the retrieval loss and the text encoder from the framework for the text generation stage and connect the pretrained vision Transformer to the language model. We use Cross Entropy loss and leverage the groundtruth box annotations to supervise the activation map in the bottleneck. We train the text generation stage for 50 epochs with Bert’s implementation of Adam optimizer settings (see Tab. 11).

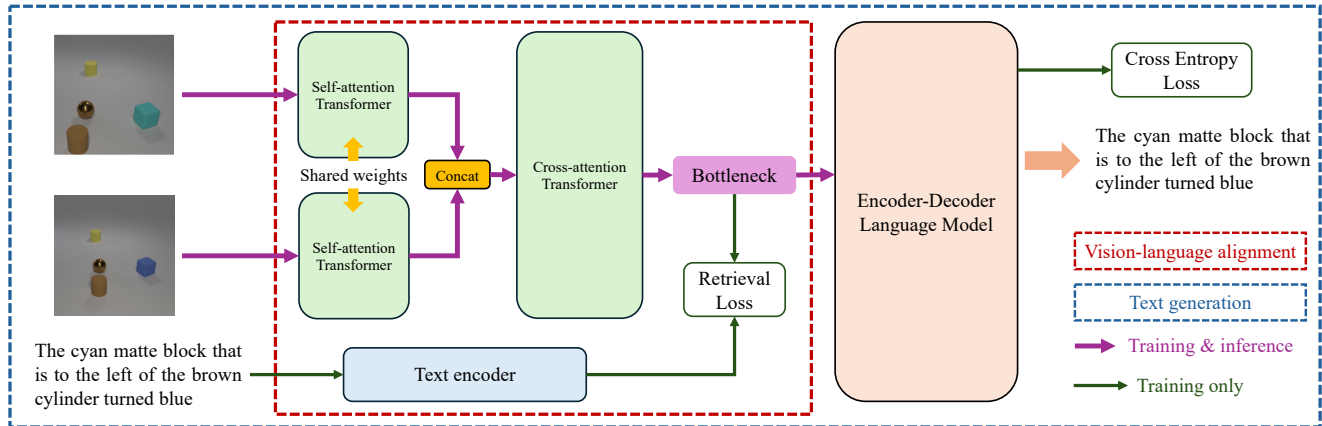


Figure 9. We use a two-stage training method for Image Difference Captioning. First, the visual embeddings extracted from the image pair in the bottleneck are aligned with the textual embeddings of the captions. In the second stage, we use a Cross Entropy loss to predict the next token.

Table 10. Vision-language alignment recipe for TAB4IDC.

Config	Value
Optimizer	Adam
Base LR	$1e^{-4}$
Scheduler	cosine decay [37]
Weight decay	0.2
Momentum	$\beta_1 = 0.9, \beta_2 = 0.98$
epsilon	$1e^{-6}$
Batch size	128
Warmup proportion	0.1
Training epochs	12

Table 11. Text generation recipe for TAB4IDC.

Config	Value
Optimizer	Adam
Base LR	$1e^{-4}$
Scheduler	linear decay
Weight decay	0.01
Momentum	$\beta_1 = 0.9, \beta_2 = 0.999$
epsilon	$1e^{-6}$
Batch size	64
Warmup proportion	0.1
Training epochs	50
Max words	32

## B. Attention visualization details

```
import cv2
import numpy as np

def resize_map(attention_map=None, input_size=(480, 320)):
    resized_map = cv2.resize(attention_map.astype(np.uint8), input_size, interpolation=cv2.INTER_CUBIC)

    return resized_map
```

Figure 10. Prior works [23, 47] use cubic interpolation to resize the attention maps that lead to smooth edges in the heatmap. Yet, it also results in peak values over image patches that have near zero attention values.

```
import cv2
import numpy as np

def resize_map(attention_map=None, input_size=(480, 320)):
    resized_map = cv2.resize(attention_map.astype(np.float32), input_size, interpolation=cv2.
    INTER_NEAREST)

    return resized_map
```

Figure 11. In our visualization paradigm, we replace the interpolation method to the nearest neighbor such that the resized attention has fewer nonzero values.

## C. Generating groundtruth captions for OpenImages-I

We have access to all the inpainted object names in OpenImages-I [43], and we generate multiple sentences describing a particular change using templates listed in Tab. 12.

Pair type	Caption template
Add	the ... has appeared
	the ... has been newly placed
	the ... has been added
Drop	the ... has disappeared
	the ... is missing
	the ... is gone
	the ... is no longer there
No-change	no change was made
	there is no change
	the two scenes seem identical
	the scene is the same as before
	the scene remains the same
	nothing has changed
	nothing was modified
	no change has occurred
	there is no difference

Table 12. We follow [47] and use the caption templates to generate groundtruth change captions

## D. STD additional results

### D.1. Localization

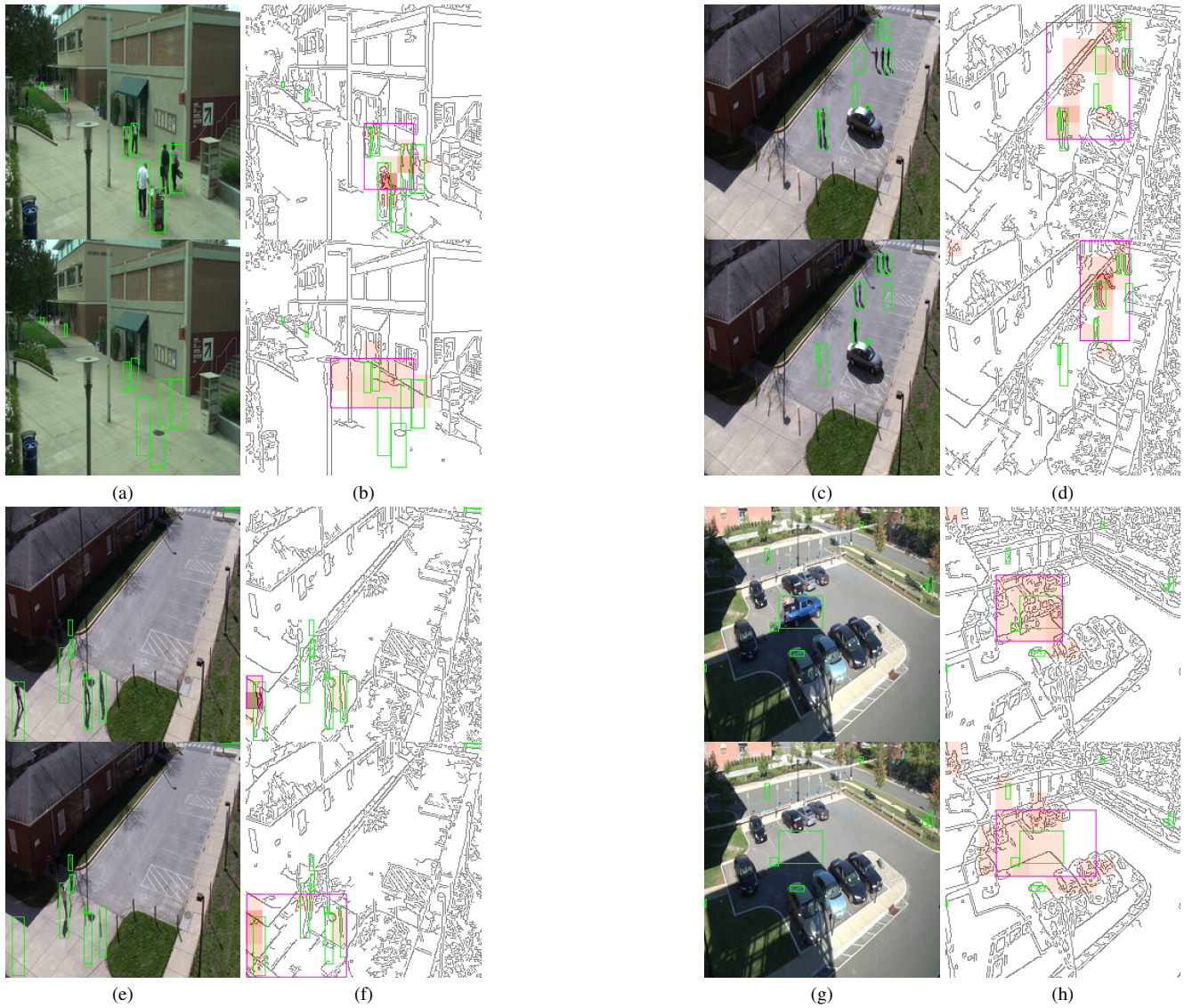


Figure 12. TAB's change localization on STD with B/16. STD contains images with multiple changes, which naturally leads to lower values in the attention maps.

## E. OpenImages-I additional results

### E.1. Correcting the attention map for change pairs

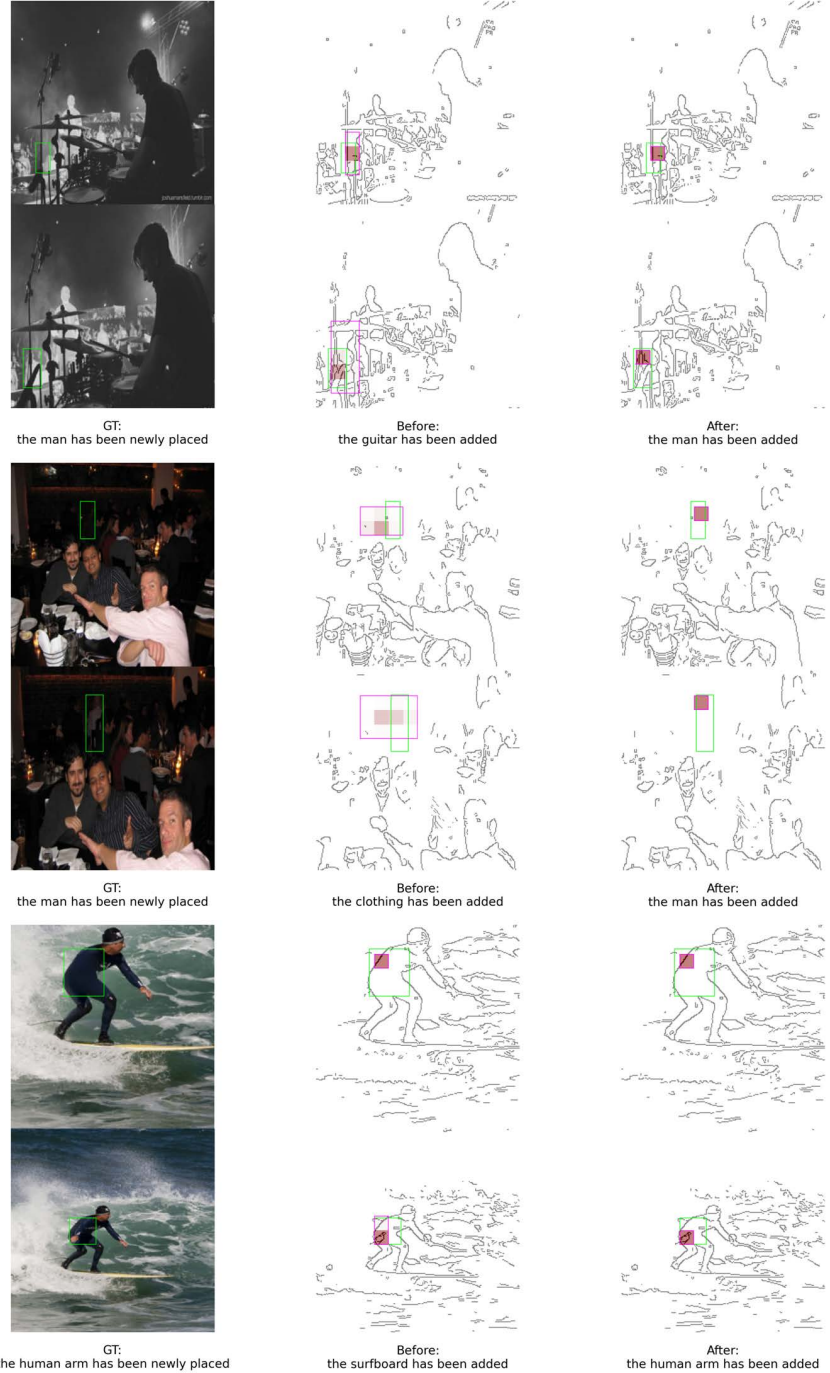


Figure 13. Editing the attention map in TAB with B/16 helps the VLM to caption the changes more accurately.



Figure 14. Editing the attention map in TAB with B/16



Figure 15. Editing the attention map in TAB with B/16

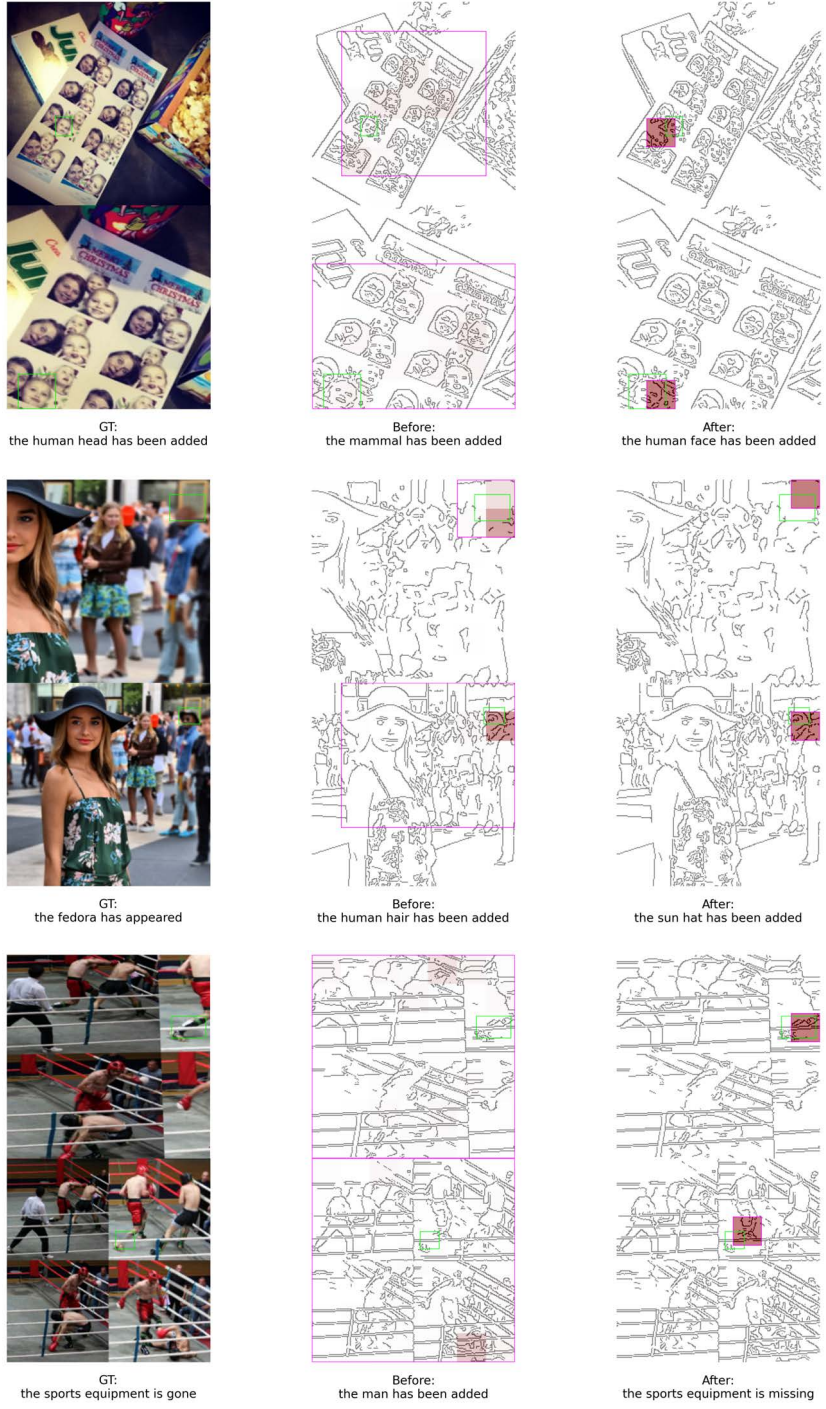


Figure 16. Editing the attention map in TAB with B/32



Figure 17. Editing the attention map in TAB with B/32

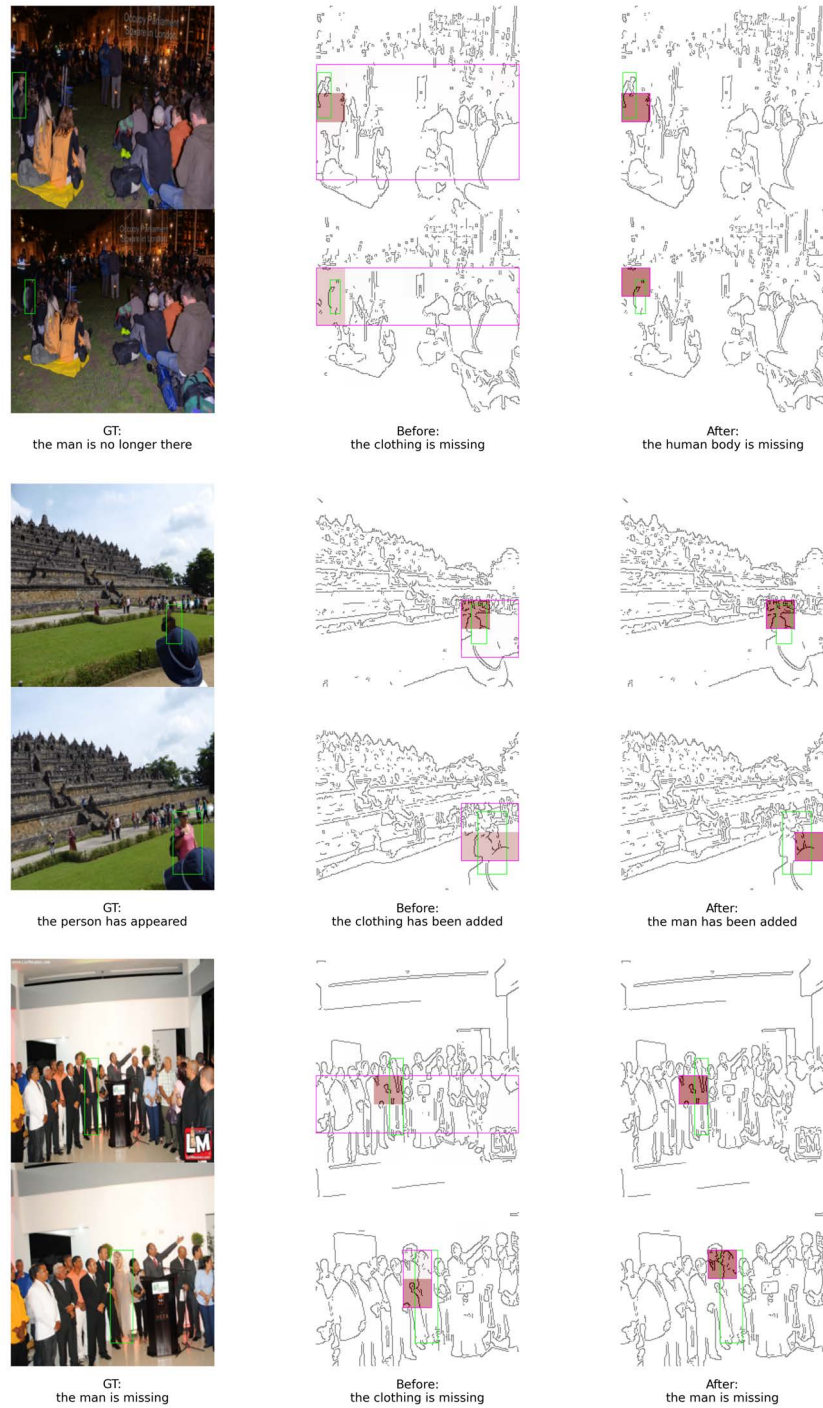


Figure 18. Editing the attention map in TAB with B/32.

## F. CLEVR-Change additional results

### F.1. Captioning and Localization

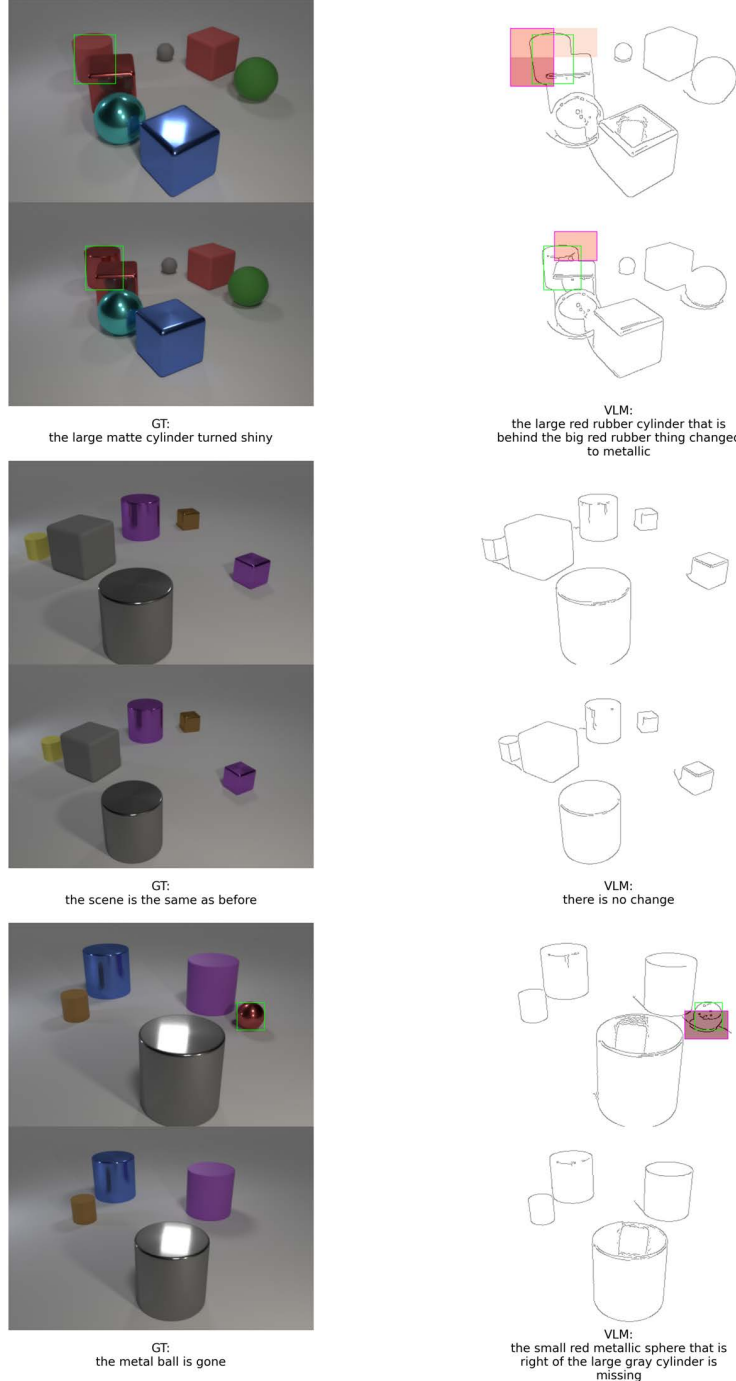
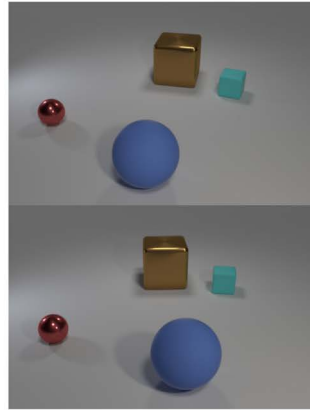
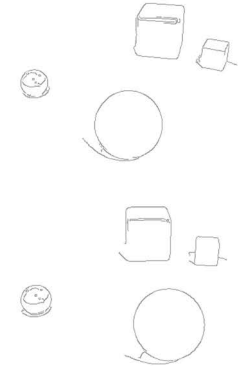


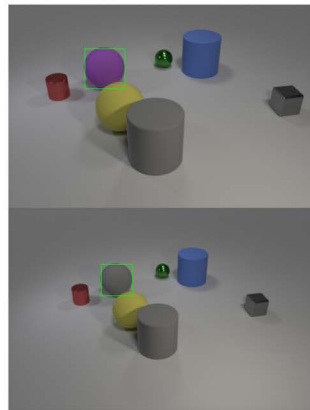
Figure 19. Captioning: TAB4IDC with B/32



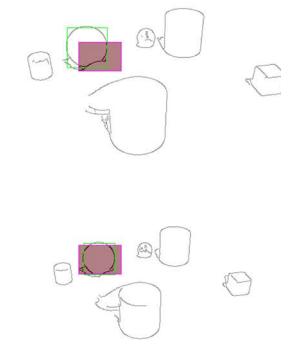
GT:  
the scene is the same as before



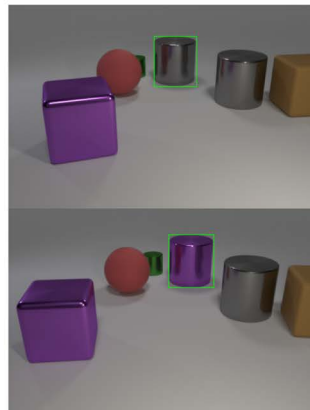
VLM:  
there is no change



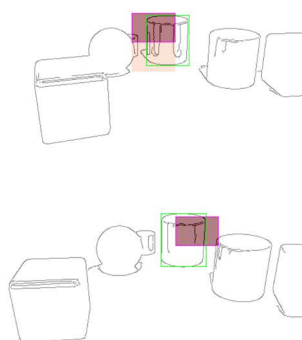
GT:  
the big purple object became gray



VLM:  
the purple rubber thing became gray

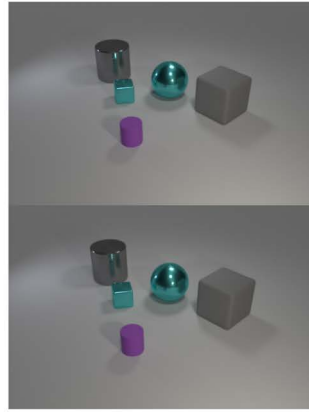


GT:  
the big gray metal cylinder behind the  
red matte object changed to purple

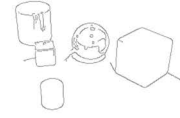


VLM:  
the big gray metallic cylinder that is  
behind the big brown rubber thing became  
purple

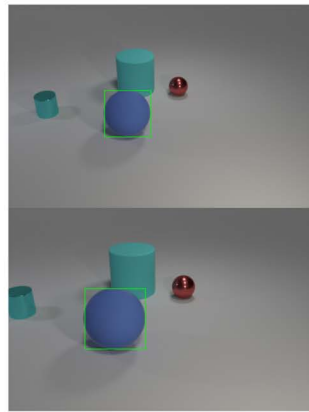
Figure 20. Captioning: TAB4IDC with B/32



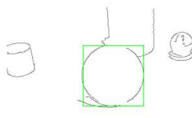
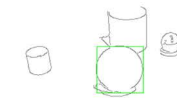
GT:  
the two scenes seem identical



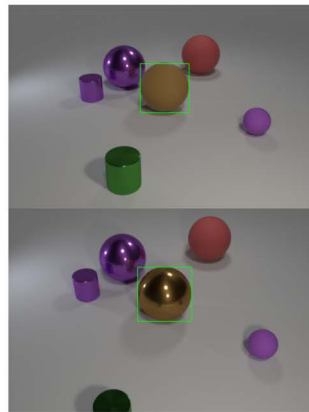
VLM:  
there is no change



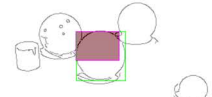
GT:  
the rubber sphere changed its location



VLM:  
there is no change

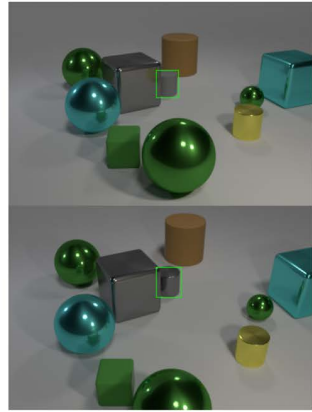


GT:  
the big brown ball changed to metallic

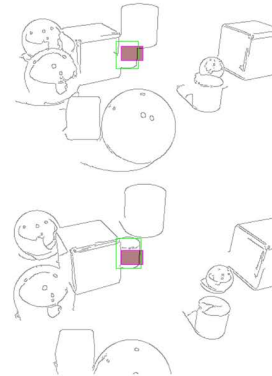


VLM:  
the large brown rubber sphere that is  
in front of the big purple rubber  
thing became shiny

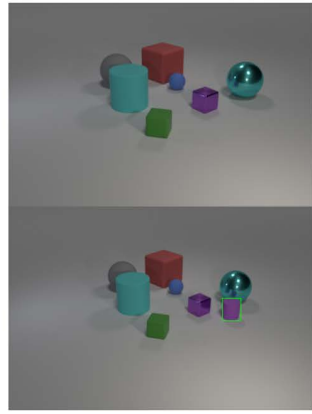
Figure 21. Captioning: TAB4IDC with B/32



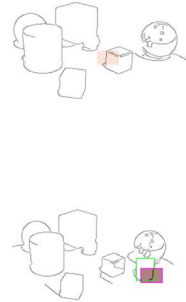
GT:  
the gray cylinder changed to shiny



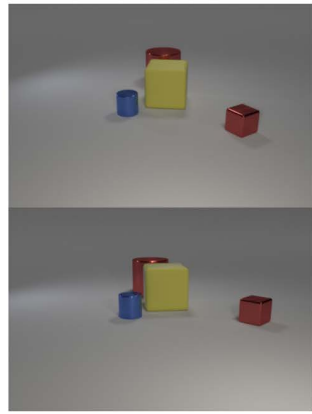
VLM:  
the tiny gray matte cylinder that is  
behind the small yellow cylinder changed to  
metallic



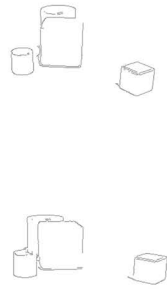
GT:  
the small cylinder has been newly placed



VLM:  
the tiny purple matte sphere that is  
to the right of the big green  
matte object has been added

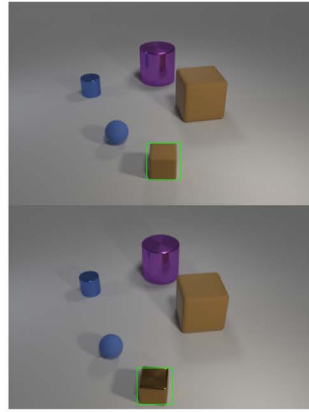


GT:  
the scene is the same as before

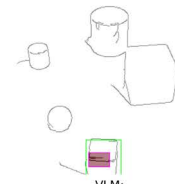
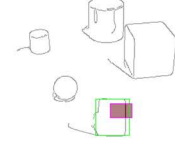


VLM:  
there is no change

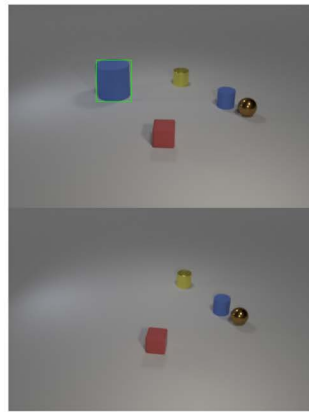
Figure 22. Captioning: TAB4IDC with B/16



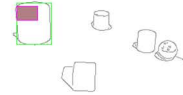
GT:  
the small brown cube became shiny



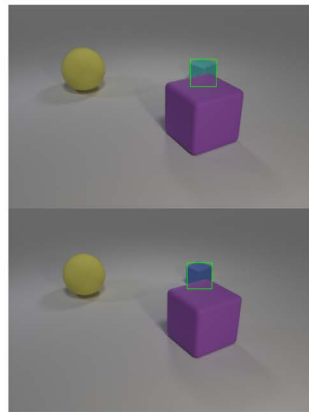
VLM:  
the tiny brown matte block that is  
in front of the small yellow matte  
object changed to metallic



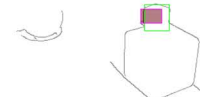
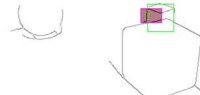
GT:  
the big matte cylinder is missing



VLM:  
the big blue matte cylinder that is  
left of the small blue matte object  
is gone

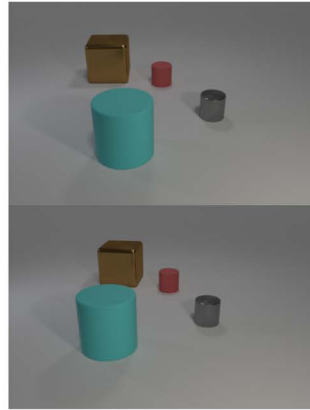


GT:  
the small object turned blue

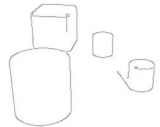
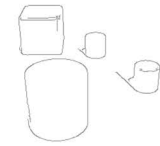


VLM:  
the tiny cyan matte block that is  
behind the small yellow cylinder changed to  
blue

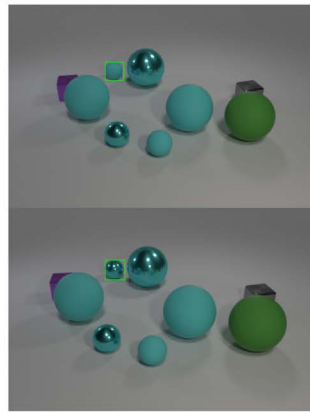
Figure 23. Captioning: TAB4IDC with B/16



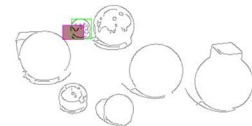
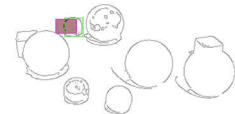
GT:  
nothing has changed



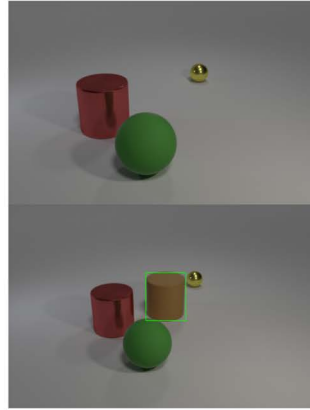
VLM:  
there is no change



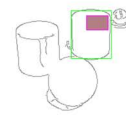
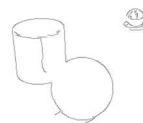
GT:  
the small cyan matte sphere behind the tiny gray metal cube became metal



VLM:  
the tiny cyan rubber ball that is behind the tiny yellow cylinder changed to metallic



GT:  
the rubber cylinder has been newly placed



VLM:  
the large brown matte cylinder that is behind the big red metal object has been added

Figure 24. Captioning: TAB4IDC with B/16

## F.2. Correcting the attention map for change pairs

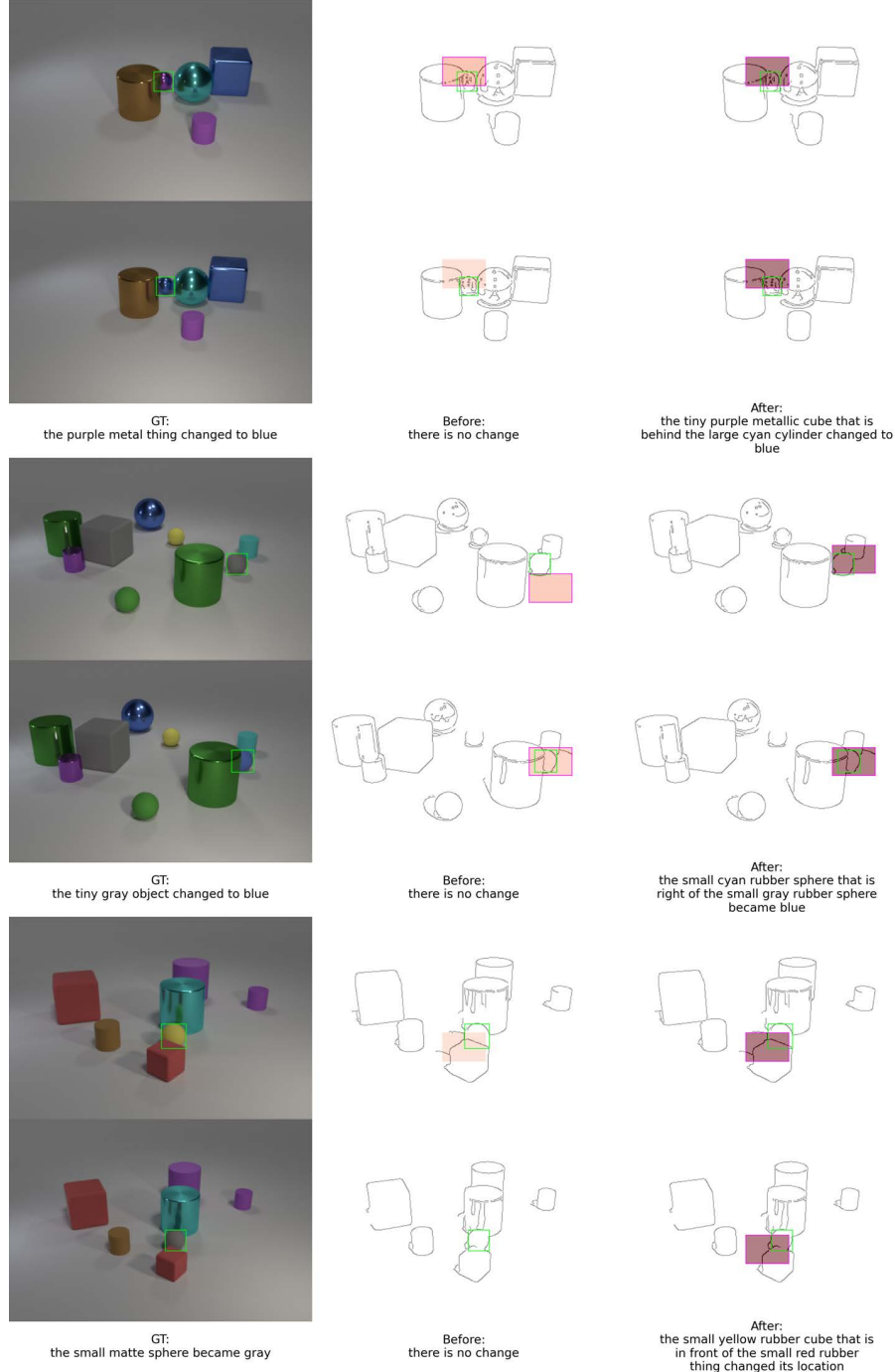


Figure 25. Editing the attention map in TAB with B/32

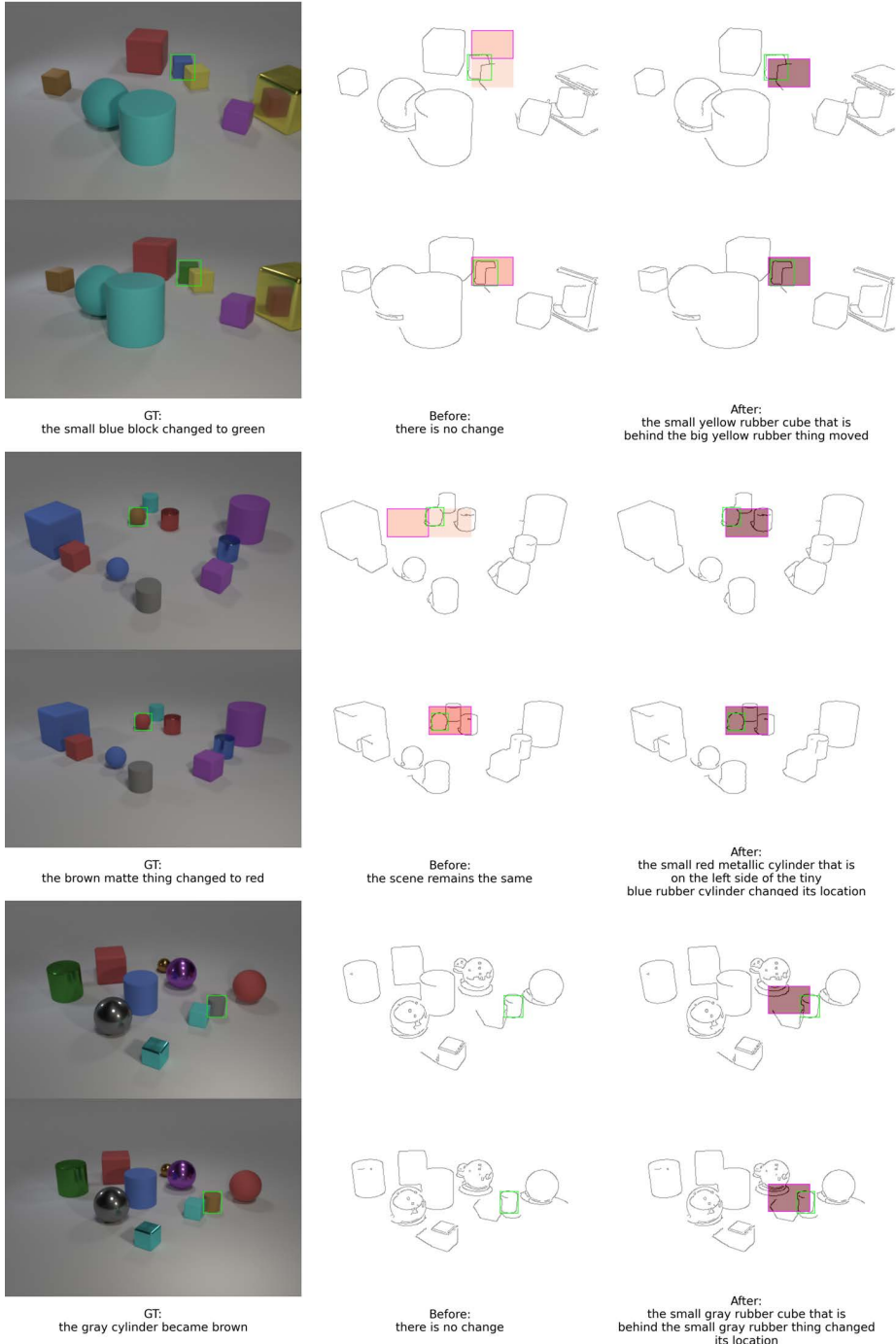


Figure 26. Editing the attention map in TAB with B/32

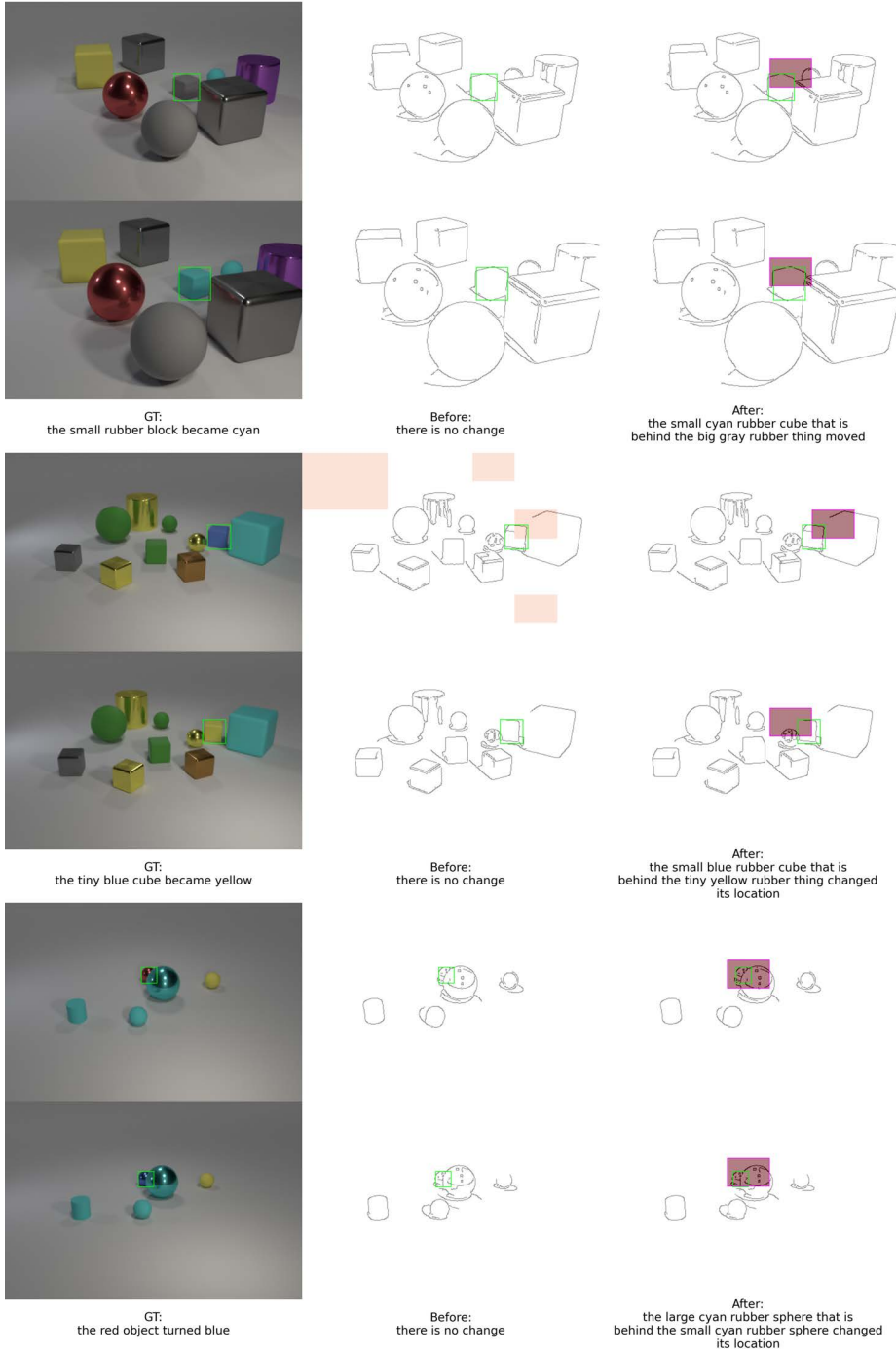


Figure 27. Editing the attention map in TAB with B/32

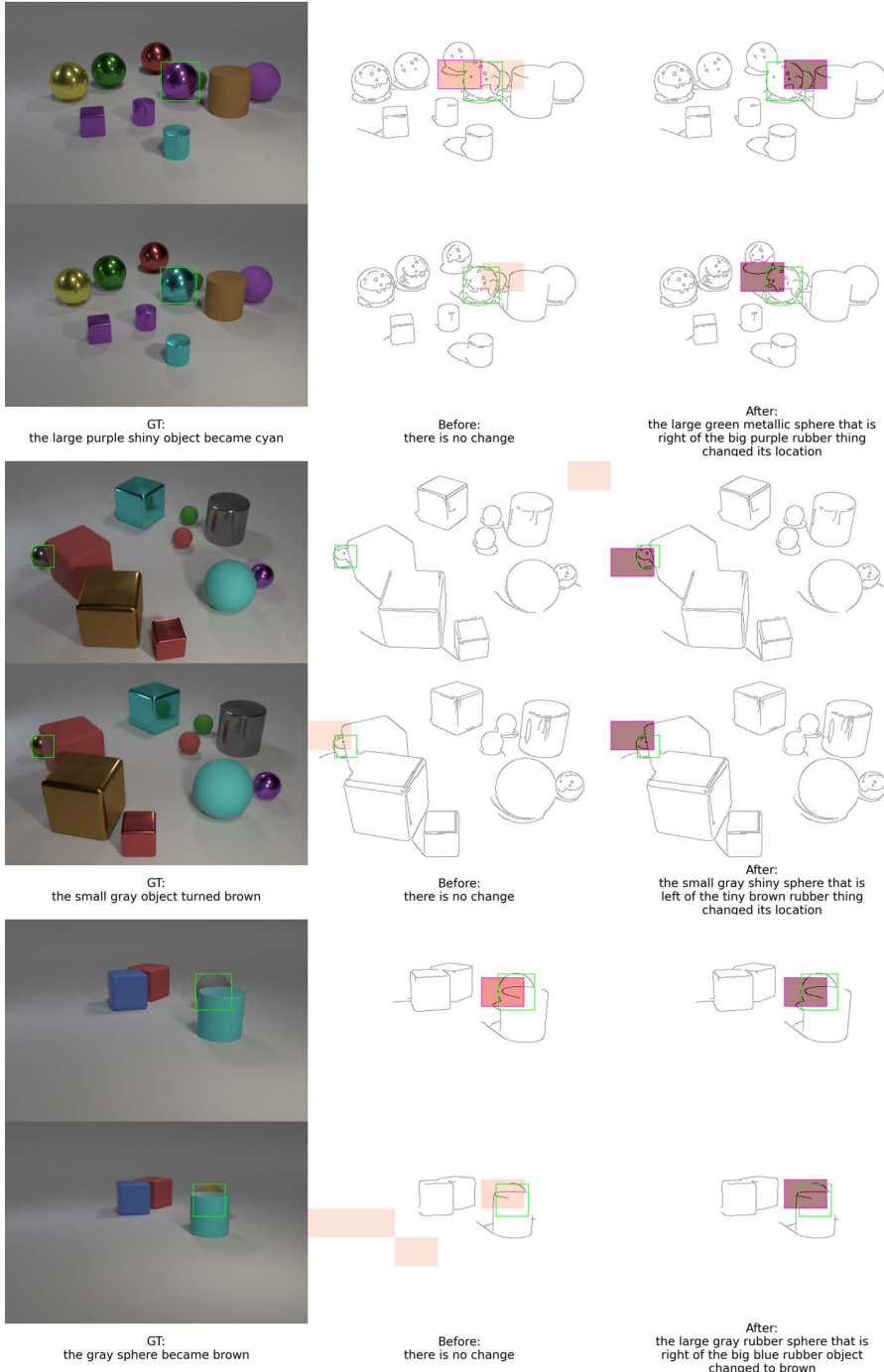


Figure 28. Editing the attention map in TAB with B/32

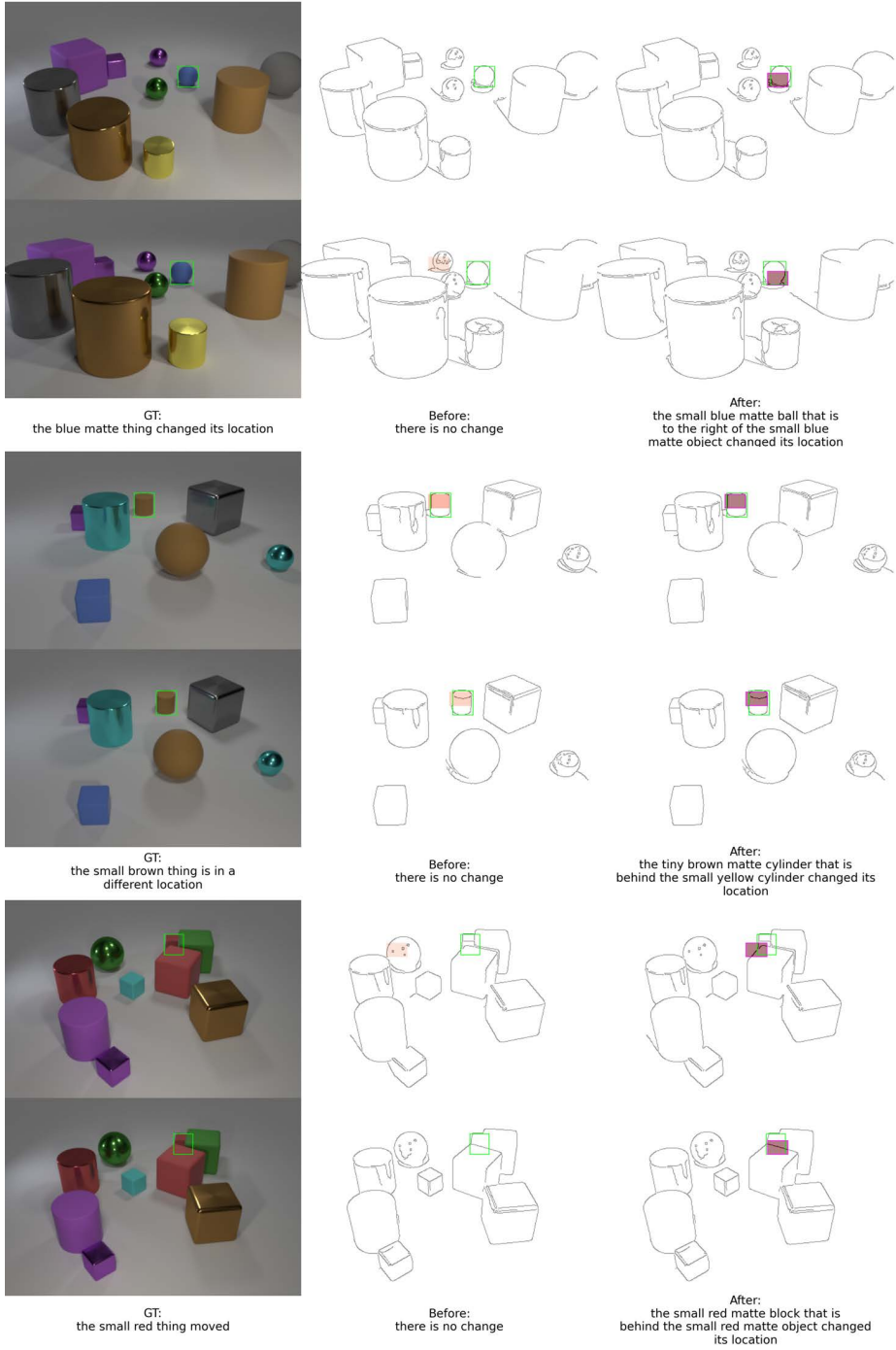


Figure 29. Editing the attention map in TAB with B/16

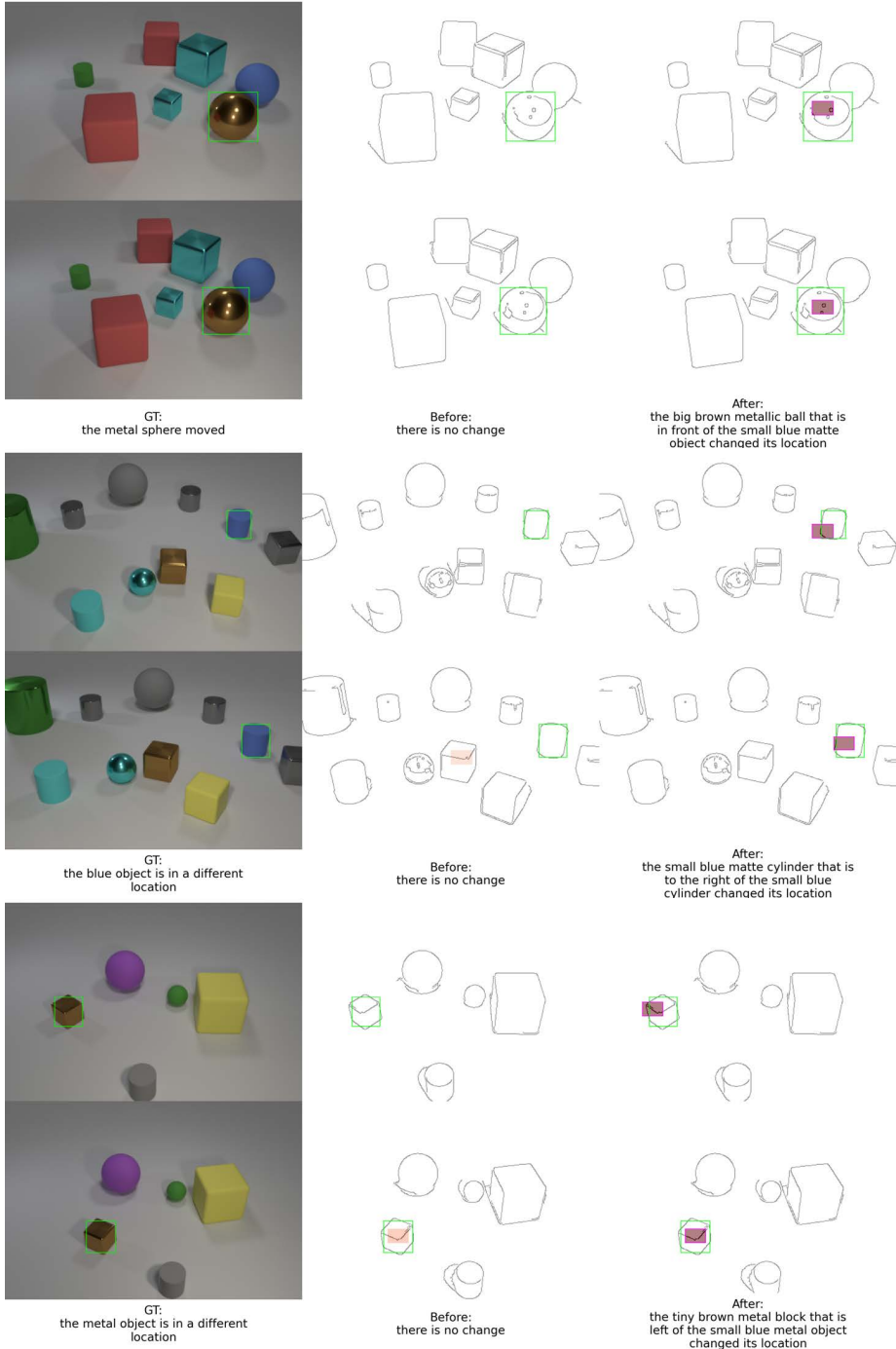


Figure 30. Editing the attention map in TAB with B/16

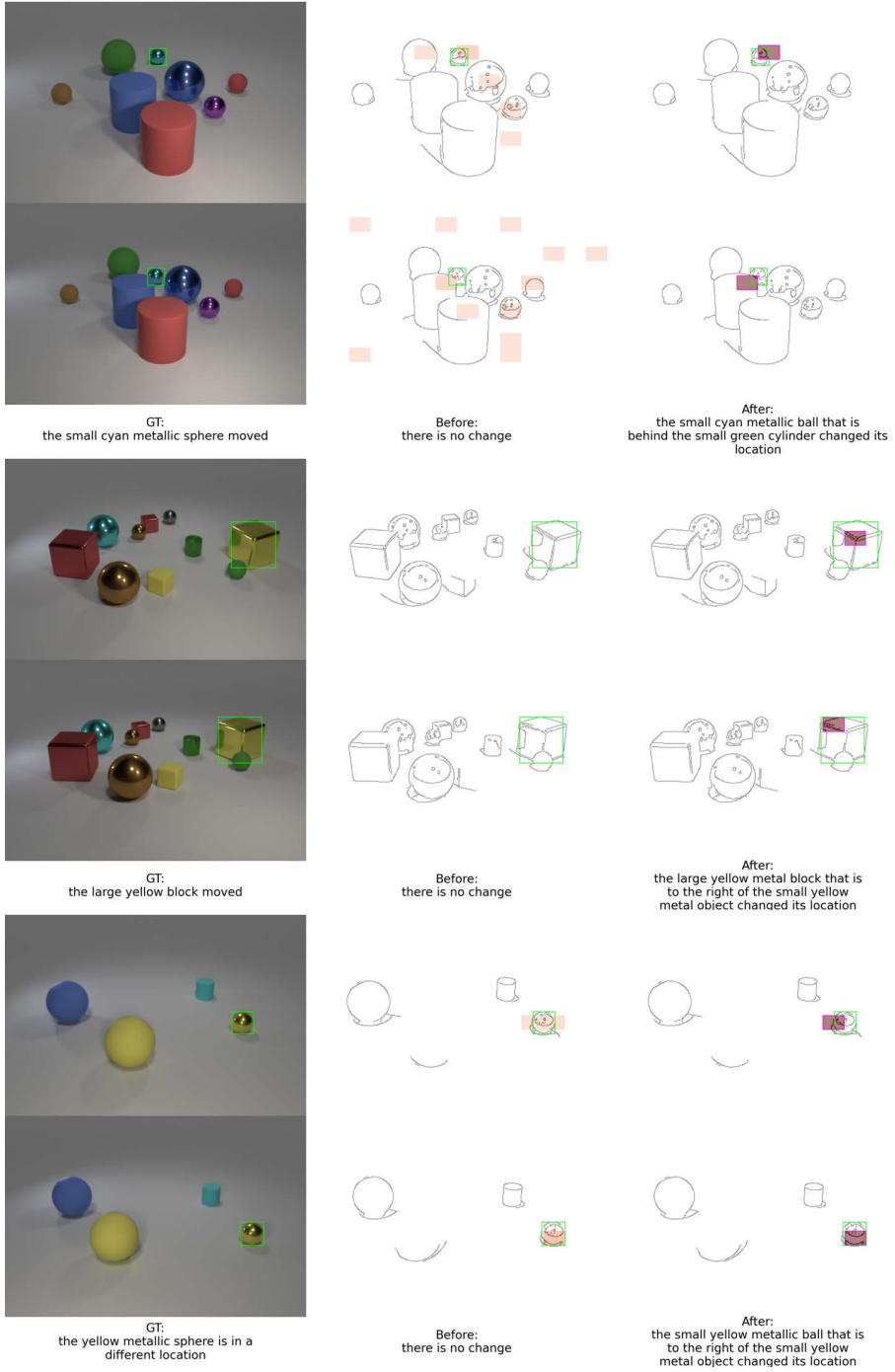


Figure 31. Editing the attention map in TAB with B/16

### F.3. Zeroing the attention map for no-change pairs

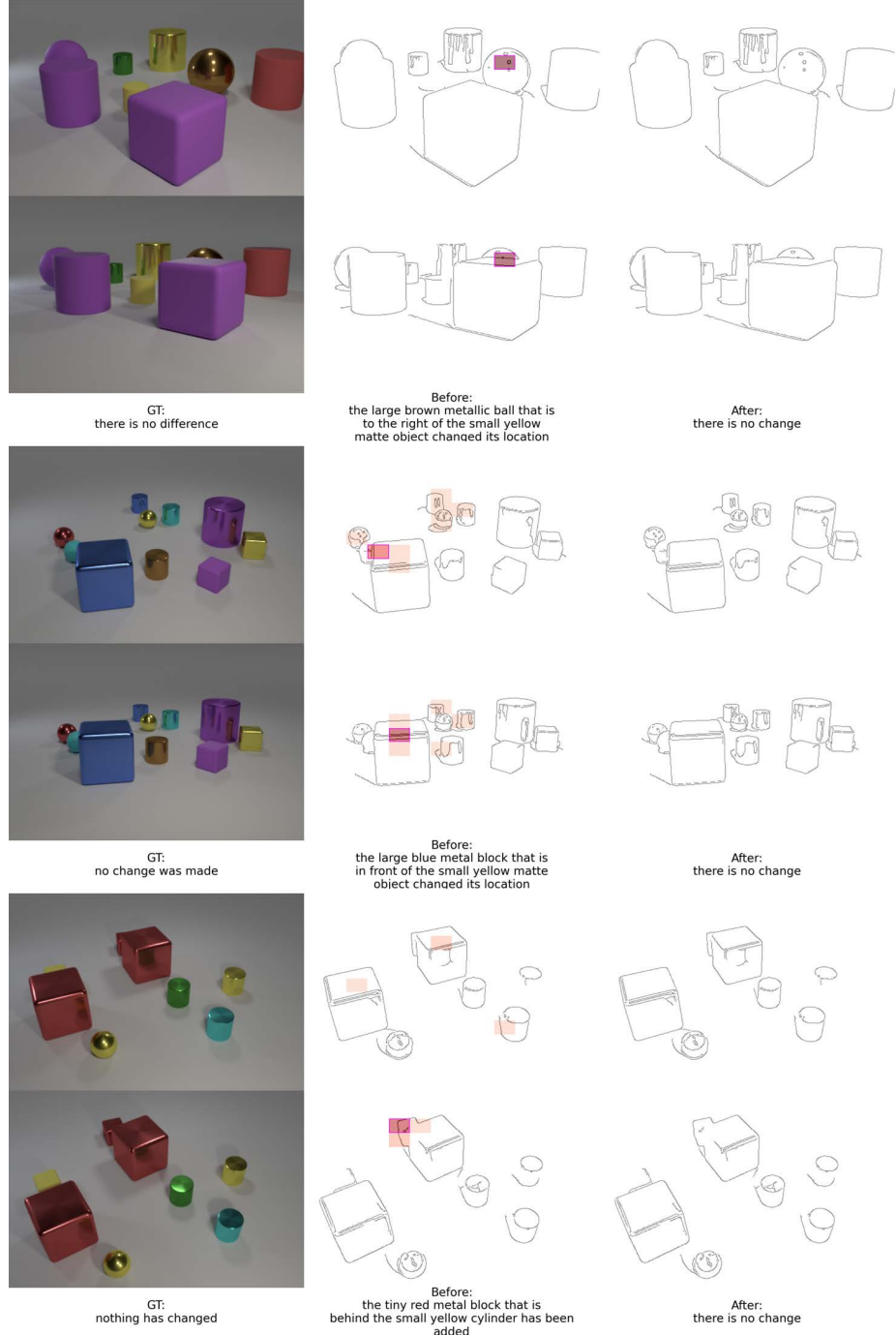


Figure 32. Editing the attention map in TAB with B/16

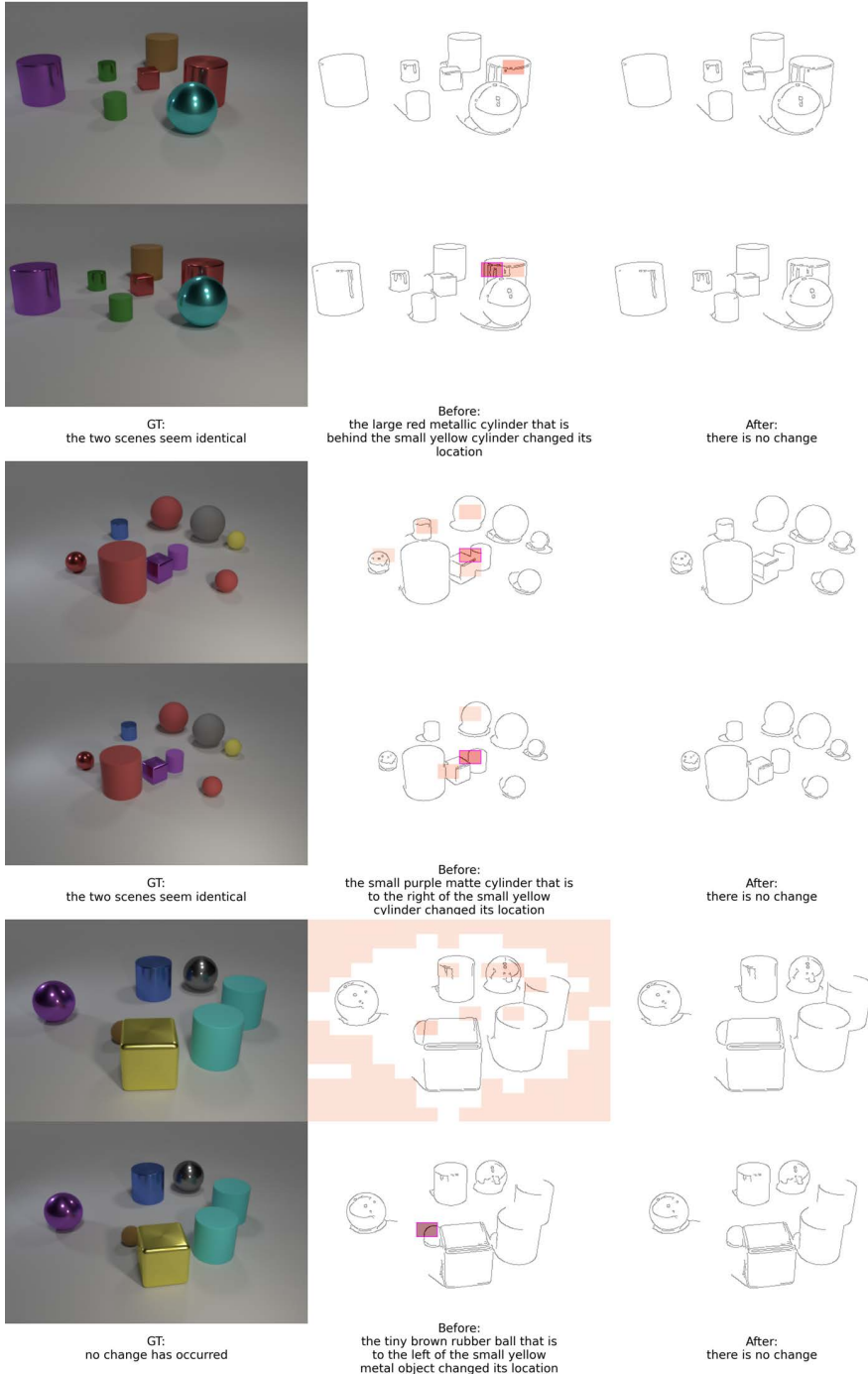


Figure 33. Editing the attention map in TAB with B/16

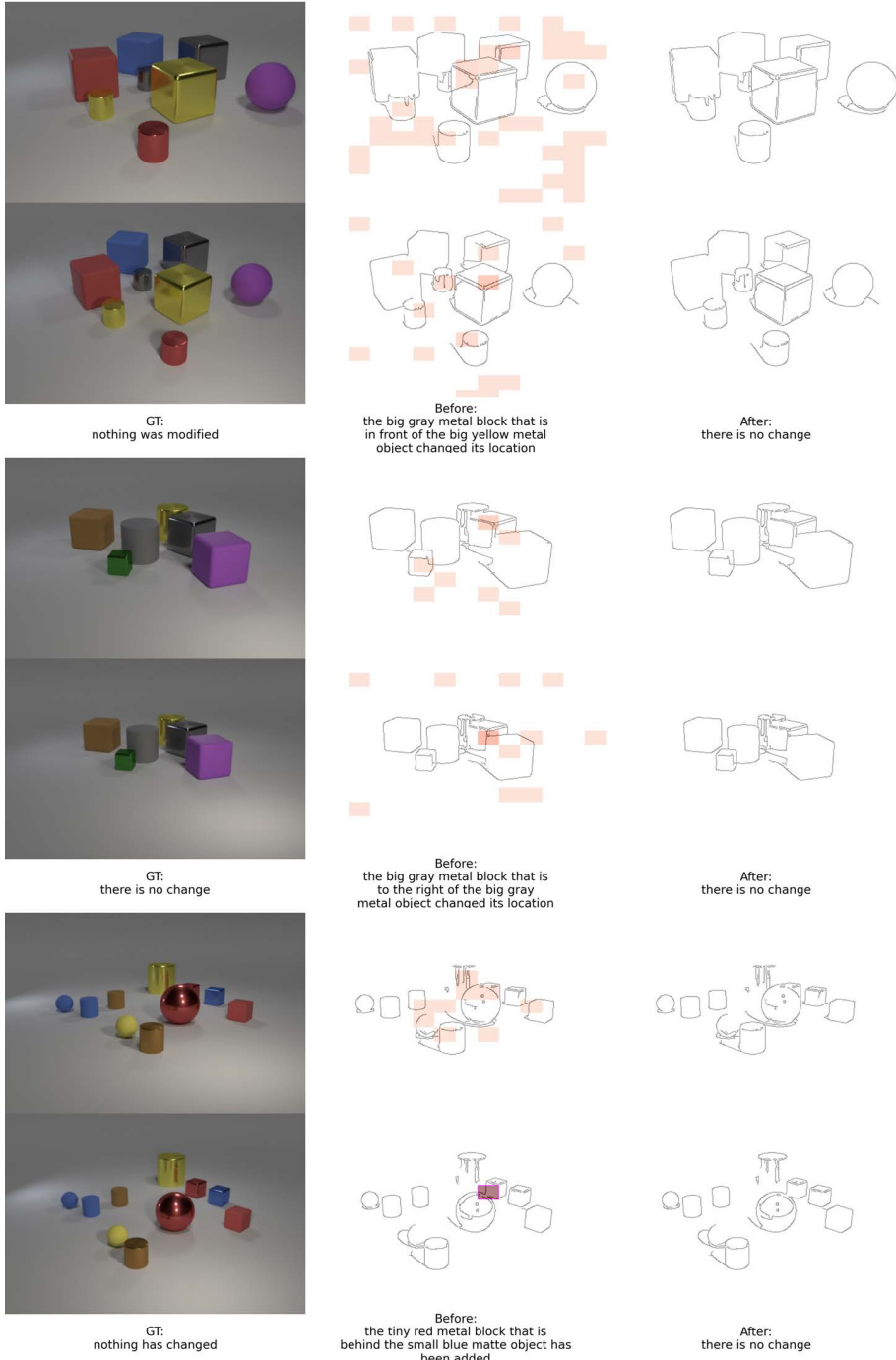


Figure 34. Editing the attention map in TAB with B/16

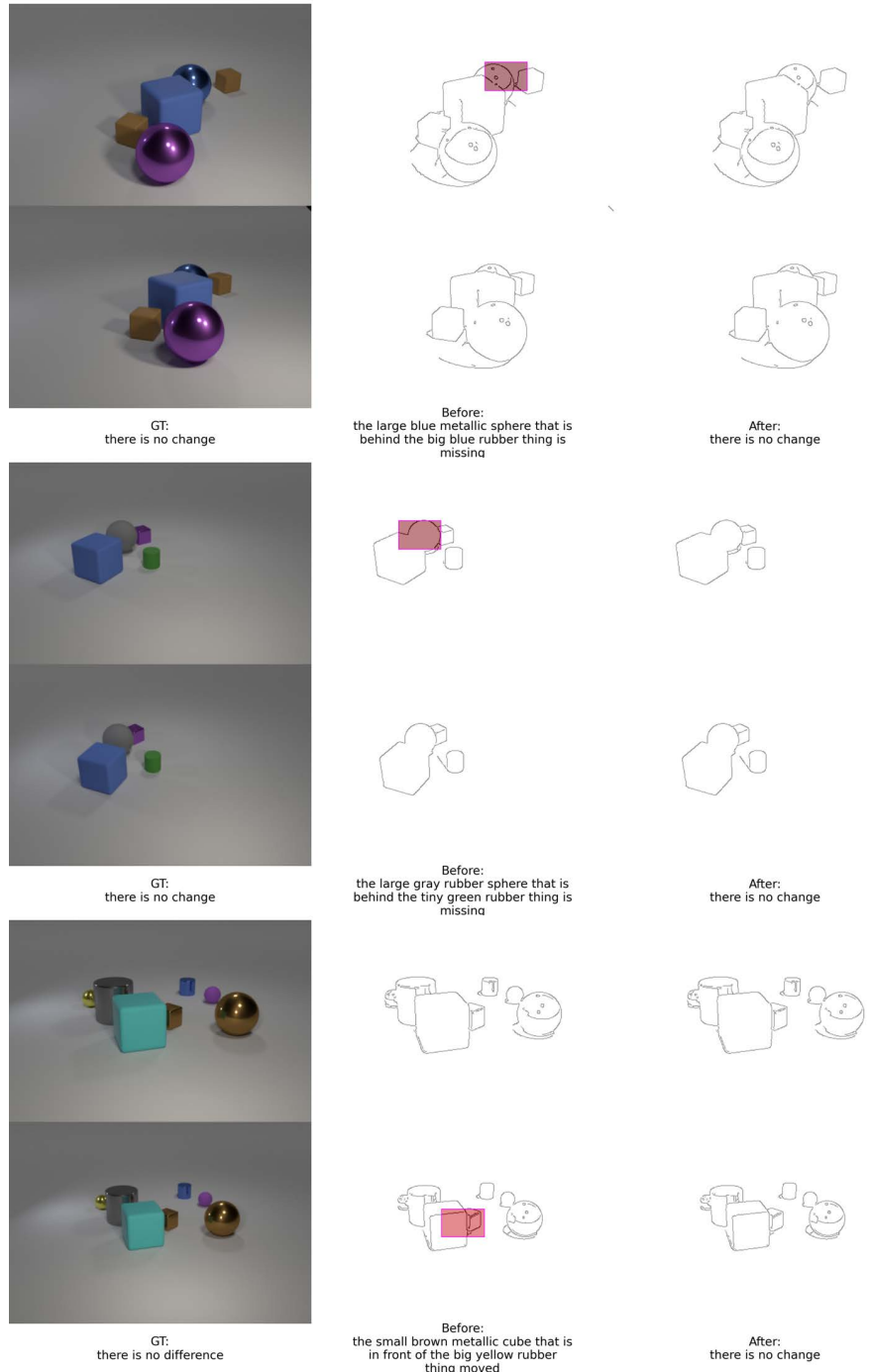


Figure 35. Editing the attention map in TAB with B/16

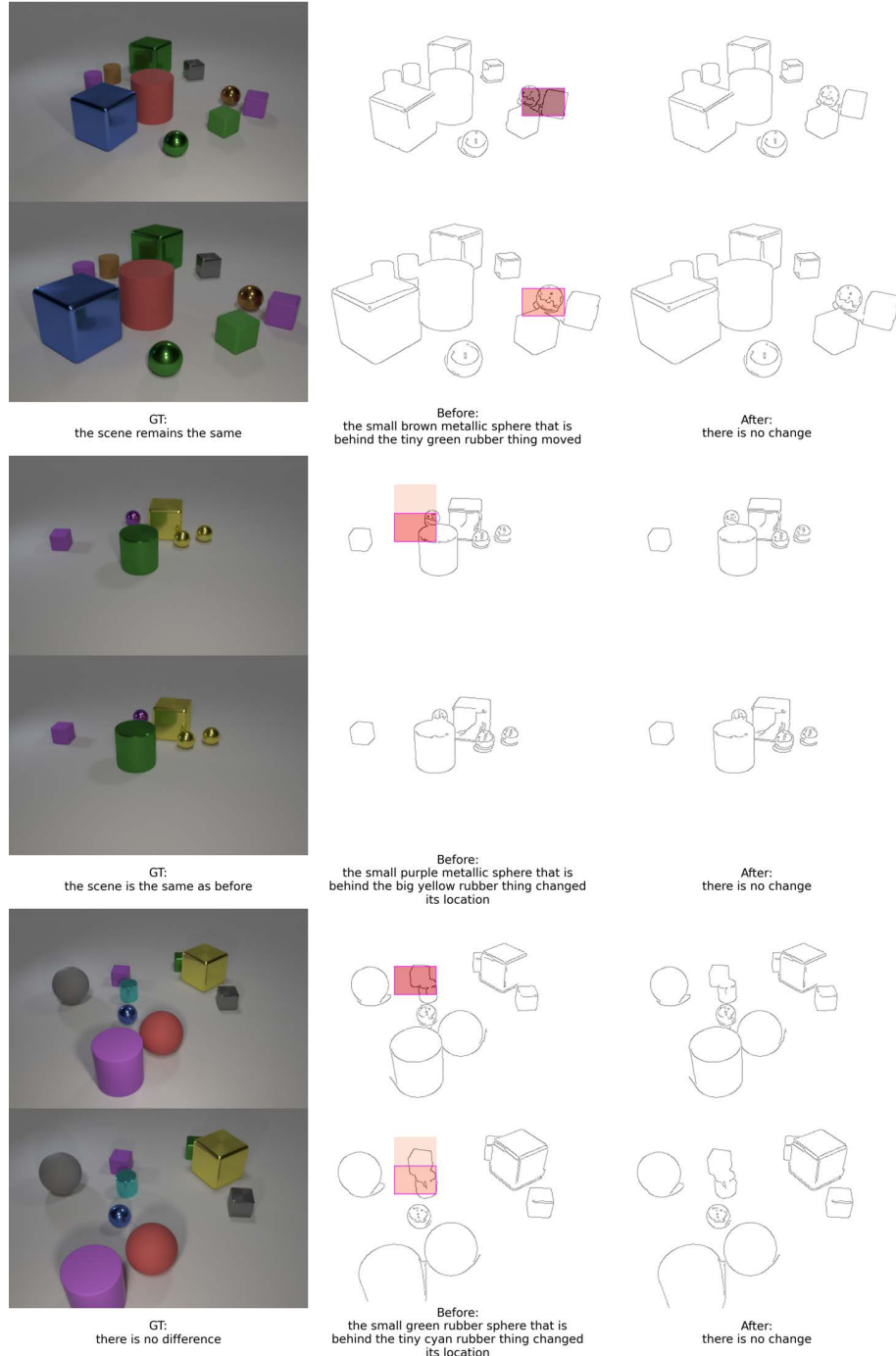


Figure 36. Editing the attention map in TAB with B/16

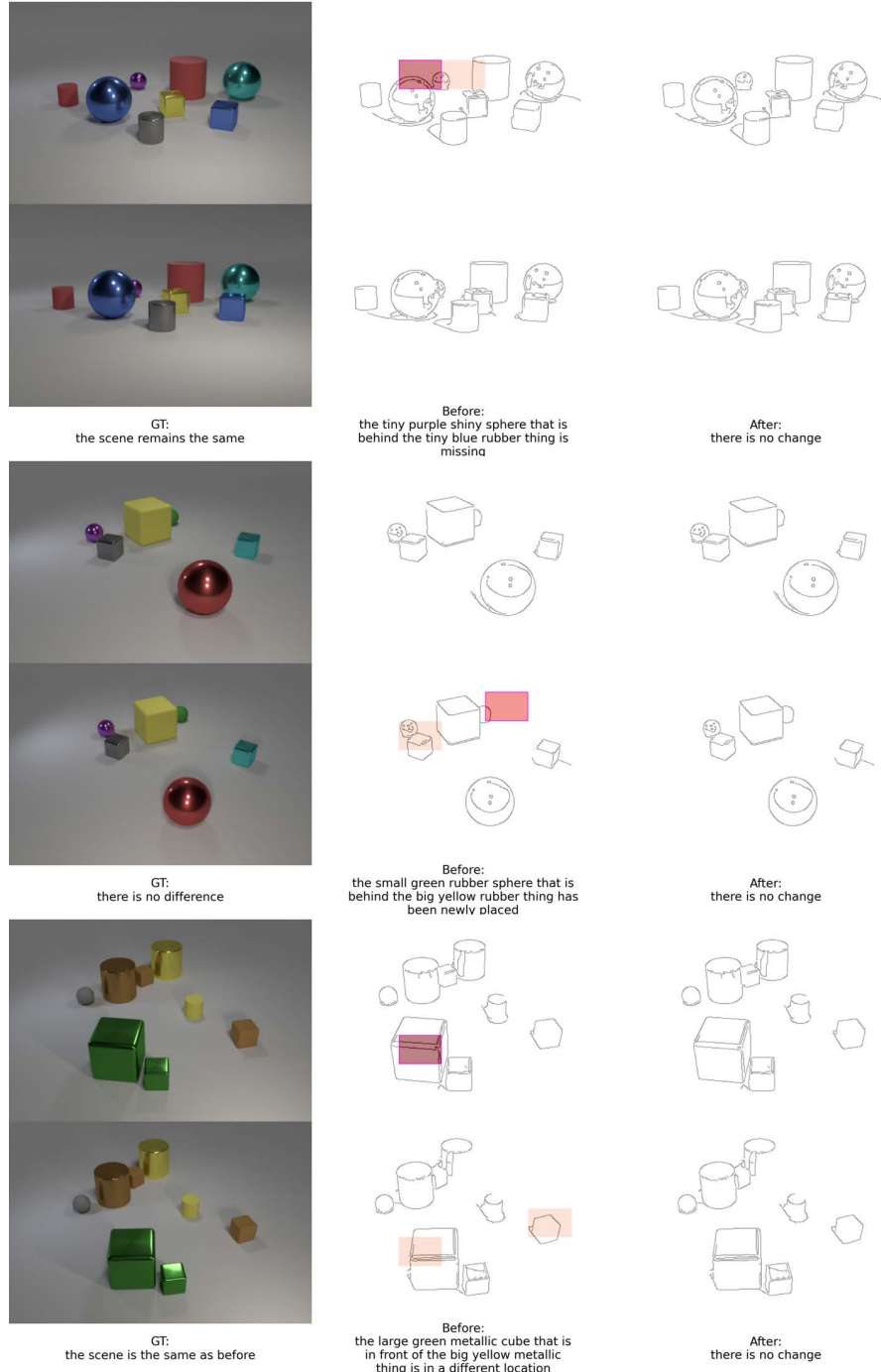


Figure 37. Editing the attention map in TAB with B/16